ARTIFICIAL BIO-INSPIRED HYBRID MUSCLE

A Final Year Project Report

Presented to

SCHOOL OF MECHANICAL & MANUFACTURING ENGINEERING

Department of Mechanical Engineering

NUST

ISLAMABAD, PAKISTAN

In Partial Fulfillment
of the Requirements for the Degree of
Bachelors of Mechanical Engineering

by

Fahd Imtiaz
Ibrahim Bin Yasir
Muhammad Umer Khan Niazi

July 2018

EXAMINATION COMMITTEE

We hereby recommend that the final year project report prepared under our supervision by:

Fahd Imtiaz	NUST20143350711114F
Ibrahim Bin Yasir	NUST20143344111114F
Muhammad Umer Khan Niazi	NUST20143299011114F

Titled: "**ARTIFICIAL BIO-INSPIRED HYBRID MUSCLE**" be accepted in partial fulfillment of the requirements for the award of **Bachelor in Mechanical Engineering** degree.

Supervisor: Dr Yasir Ayaz
SMME, NUST

Dated: _____

Committee Member: AP Sara Babar Sial
SMME, NUST

Dated: _____

Committee Member: Lec Hamza Asif
SMME, NUST

Dated: _____

_____ _____

(Head of Department) (Date)

COUNTERSIGNED

Dated: _____ _____

(Dean / Principal)

ABSTRACT

Soft bodied actuator mechanisms exist as an alternative to Rigid bodied actuator mechanisms for applications where smoother actuation rates, better power to weight ratios and conformability to shape are required. But since they exist on the opposite end of the spectrum they lack in repeatability, structural rigidity and actuation power. After performing a detailed literature review we established this design in which a hybrid approach was used to get the best of both worlds. By integrating rigid elements in the form of shells with a soft elastomeric tube, a hybrid actuator was formed having better power to weight ratio and smoother actuation rates when compared to rigid bodied actuator mechanisms and better structural rigidity, repeatability and actuation power when compared to rigid bodied mechanisms. A mathematical model was developed by solving the soft and rigid elements separately to get the end effector position, forces and torques. This model was conferred by doing FEM Simulation for a simpler version of the design. An experimental prototype was then developed for verification using materials chosen by the literature review performed earlier. Simple tests were done on the prototype to determine its working specifications. Finally, future work was discussed and some specific applications were demonstrated.

PREFACE

With the increase in the use of Robotic Systems in our daily lives. There has been a need for safer physical human robot interactions (pHRI). Although soft bodied actuator systems fulfill this need due to their smoother actuation rates and as the name implies soft bodies. However, for specific applications where better repeatability, control and greater actuation power are required another type of system was needed. This work proposes one such hybrid system which was inspired form the tail muscles of crustaceans specifically lobsters and combines rigid elements in the form of shells with a soft elastomeric body. This then acts as a pneumatically actuated artificial muscle. The aim of this work was to develop an actuator system iterating on the already established soft bodied actuators while trying to mitigate some of the problems that restrict their fields of application.

ACKNOWLEDGMENTS

Thanks to ALLAH Almighty, as it is due to His blessing that we have gained the knowledge and skills required to complete this project. We would also like to appreciate the support from our families.

Now we also want to express our gratitude towards our supervisor Dr. Yasar Ayaz not only for his continued support and guidance but also for the fact that he kept pushing us to go further. Similarly, we like to thank Lec Hamza Asif, Dr. Jawad Khan and Miss Sara Baber for their guidance. This project would not have been possible without them. Lastly, we would like to thank "National University of Sciences and Technology (NUST)", specifically the department of Mechanical and Manufacturing Engineering (SMME) for their support and cooperation towards our project.

ORIGINALITY REPORT

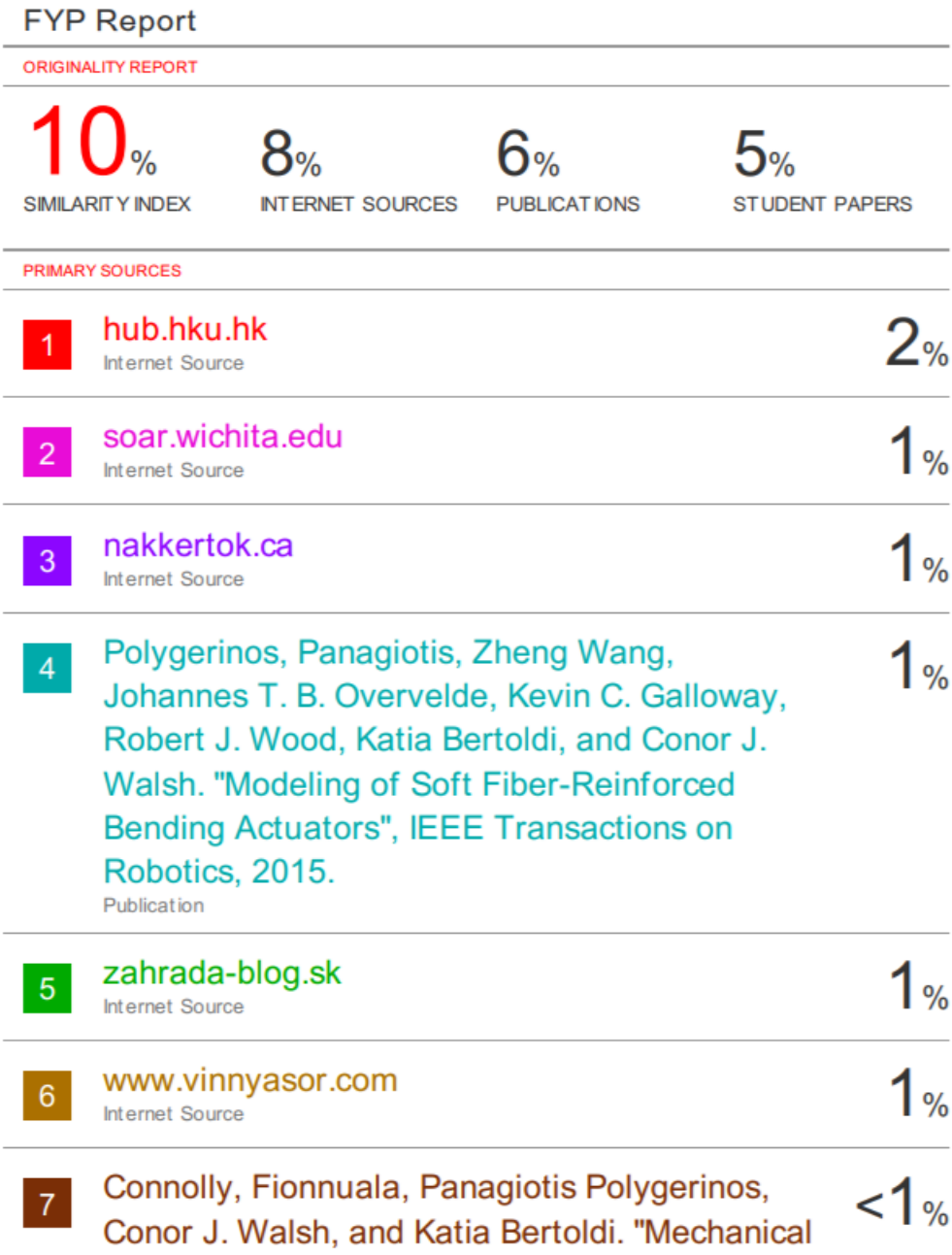

FYP Report

ORIGINALITY REPORT

10%	8%	6%	5%
SIMILARITY INDEX	INTERNET SOURCES	PUBLICATIONS	STUDENT PAPERS

PRIMARY SOURCES

1	hub.hku.hk Internet Source	2%
2	soar.wichita.edu Internet Source	1%
3	nakkertok.ca Internet Source	1%
4	Polygerinos, Panagiotis, Zheng Wang, Johannes T. B. Overvelde, Kevin C. Galloway, Robert J. Wood, Katia Bertoldi, and Conor J. Walsh. "Modeling of Soft Fiber-Reinforced Bending Actuators", IEEE Transactions on Robotics, 2015. Publication	1%
5	zahrada-blog.sk Internet Source	1%
6	www.vinnyasor.com Internet Source	1%
7	Connolly, Fionnuala, Panagiotis Polygerinos, Conor J. Walsh, and Katia Bertoldi. "Mechanical	<1%

	Programming of Soft Actuators by Varying Fiber Angle", Soft Robotics, 2015. Publication	
8	Submitted to London School of Commerce Student Paper	<1%
9	Submitted to University of Technology, Sydney Student Paper	<1%
10	Submitted to Central Queensland University Student Paper	<1%
11	repository.ntu.edu.sg Internet Source	<1%
12	Submitted to Sheffield Hallam University Student Paper	<1%
13	Ivan Kostov, Stefcho Guninski. "Determination of control sensor position in a clapper type electromagnet using FEM", 2017 15th International Conference on Electrical Machines, Drives and Power Systems (ELMA), 2017 Publication	<1%
14	eprints.qut.edu.au Internet Source	<1%
15	Submitted to The RCY Colleges & Institutes Student Paper	<1%
16	Submitted to University of Teesside	

	Student Paper	<1%
17	qspace.qu.edu.qa Internet Source	<1%
18	zh.scientific.net Internet Source	<1%
19	Yaohui Chen, Sing Le, Qiao Chu Tan, Oscar Lau, Fang Wan, Chaoyang Song. "A reconfigurable hybrid actuator with rigid and soft components", 2017 IEEE International Conference on Robotics and Automation (ICRA), 2017 Publication	<1%
20	Submitted to Argosy University Student Paper	<1%
21	documents.mx Internet Source	<1%
22	Yaohui Chen, Sing Le, Qiao Chu Tan, Oscar Lau, Chaoyang Song. "A Lobster-Inspired Hybrid Actuator With Rigid and Soft Components", Volume 5B: 41st Mechanisms and Robotics Conference, 2017 Publication	<1%
23	Mata Amritanandamayi Devi, Ganesha Udupa, Pramod Sreedharan. "A novel underactuated	<1%

multi-fingered soft robotic hand for prosthetic application", Robotics and Autonomous Systems, 2018
Publication

24	dspace.lboro.ac.uk Internet Source	<1%
25	Advances in Intelligent Systems and Computing, 2017. Publication	<1%
26	smme.nust.edu.pk Internet Source	<1%
27	doras.dcu.ie Internet Source	<1%
28	bertoldi.seas.harvard.edu Internet Source	<1%
29	researchbank.rmit.edu.au Internet Source	<1%
30	bidsets.publicworks.houstontx.gov Internet Source	<1%
31	rspa.royalsocietypublishing.org Internet Source	<1%
32	Gerboni, Giada, Tommaso Ranzani, Alessandro Diodato, Gastone Ciuti, Matteo Cianchetti, and Arianna Menciassi. "Modular soft mechatronic manipulator for minimally	<1%

	invasive surgery (MIS): overall architecture and development of a fully integrated soft module", Meccanica, 2015. Publication	
33	lift-kits-direct.com Internet Source	<1%
34	biodesign.seas.harvard.edu Internet Source	<1%
35	hal.archives-ouvertes.fr Internet Source	<1%
36	tel.archives-ouvertes.fr Internet Source	<1%
37	open.uct.ac.za Internet Source	<1%
38	www.minfo.se Internet Source	<1%
39	Zhisheng Zhang, Qi Zhang, Min Dai, Xiqi Ding, Zhijie Xia. "Modeling of multi-cavity composite soft pneumatic actuators", 2017 24th International Conference on Mechatronics and Machine Vision in Practice (M2VIP), 2017 Publication	<1%
40	Ricardo Campa, Karla Camarillo, Lina Arias. "Kinematic Modeling and Control of Robot Manipulators via Unit Quaternions: Application	<1%

to a Spherical Wrist", Proceedings of the 45th IEEE Conference on Decision and Control, 2006
Publication

Exclude quotes	On	Exclude matches	< 4 words
Exclude bibliography	On		

COPYRIGHT

School of Mechanical and Manufacturing Engineering (SMME)

NUST, H-12

Islamabad

TABLE OF CONTENTS

LIST OF TABLES

LIST OF FIGURES

ABBREVIATIONS

pHRI	Physical Human Robot Interaction
pneu-nets	Pneumatic Networks
Rehab	Rehabilitation
DH	Denavait-Hartenberg

NOMENCLATURE

v	aspect ratio (for rectangular)
a^2	cross-sectional area
M_a	Internal Torque
P_{in}	Input Pressure
W	Strain Energy
I	Invariant
E	Final Pose
a,b,t	Local geometry constants
$.\theta$	Bend Angle
S	Principle normal Stress

CHAPTER 1: INTRODUCTION

The field of traditional robotics has been explored and developed quite extensively and thoroughly. However, with robots and their hybrids becoming more and more integrated with humans in their lives, the main focus of the research has shifted from advancements in robustness, precision and efficiency in the original designs towards interactive, collaborative, physically safe and wearable applications.

1.1 Exo-Skeletons

One such field of application is that of exo-skeletons or exo-suits as they are more widely known. These exo-skeletons are exactly as their name suggests wearable robots that assist the user in performing various tasks. Although they are classified on the basis of design, actuation mechanisms etc. But mainly they are split into two categories.

1.1.1 Hard Robotics

First is the hard robotics, they are categorized on the basis of their rigid structure. They are capable of delivering high power with good efficiency and accuracy [1]. They however add extra bulk and mass to the system to the system and thus have to be carefully regulated for safe physical human robot interaction.

1.1.2 Soft Robotics

The second classification is that of soft robotics. Developed by applying bio-inspired designs to generate robotic motion and force. This type of design not only leads to smoother actuation rates but also provides high power to weight ratio. These type of robots are used mainly for grasping purposes due to their compliant nature [2]-[4].

Despite the advances already made in the field of Soft Robotics there are many areas which need work. Some of the present limitations are:

- **Lack of control:** Soft robots do not offer the same level of precise control that hard robotics offers.
- **Robustness:** Soft robots by nature are not as robust. This severely limits their usefulness.

1.2 Why we choose Soft Robotics

Soft robotics is a relatively new field in robotics. Soft robotics is rapidly growing thanks to the need for safer physical human robot interaction. Soft robotics has emerged as a means to overcome some of the limitations of rigid robotics. The aim of soft robotics is not to replace or get rid of hard robots. Soft robots are made to integrate with hard robot; both are made to complement each other.

The following are some of the areas where soft robotics is making an impact:

1.2.1 Food and Beverage

The food and beverage industry are one which is rapidly investing in soft robotics. Food items are often delicate and the soft compliant grippers which come under the field of soft robotics comply perfectly with the needs of the industry. For traditional robots made from rigid links of metal or hard plastics sensitive and precise force control is needed to manage such a delicate task. Grippers made from soft robotics make this job many times easier.

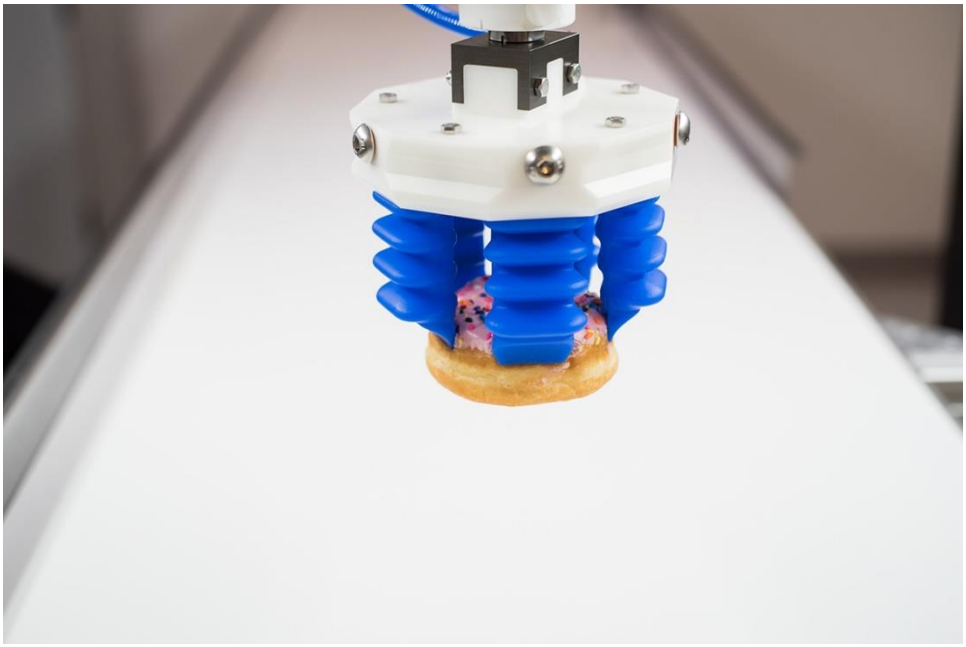

Figure 1 Image courtesy softroboticsinc.com [21]

1.2.2 Packaging and Delivery

Thanks to the adaptive nature of the flexible actuators employed in in soft robotics, soft robots are almost perfect for the packaging industry. Grippers made from soft materials can easily adapt to a variety of shapes and handle delicate items with the care they need.

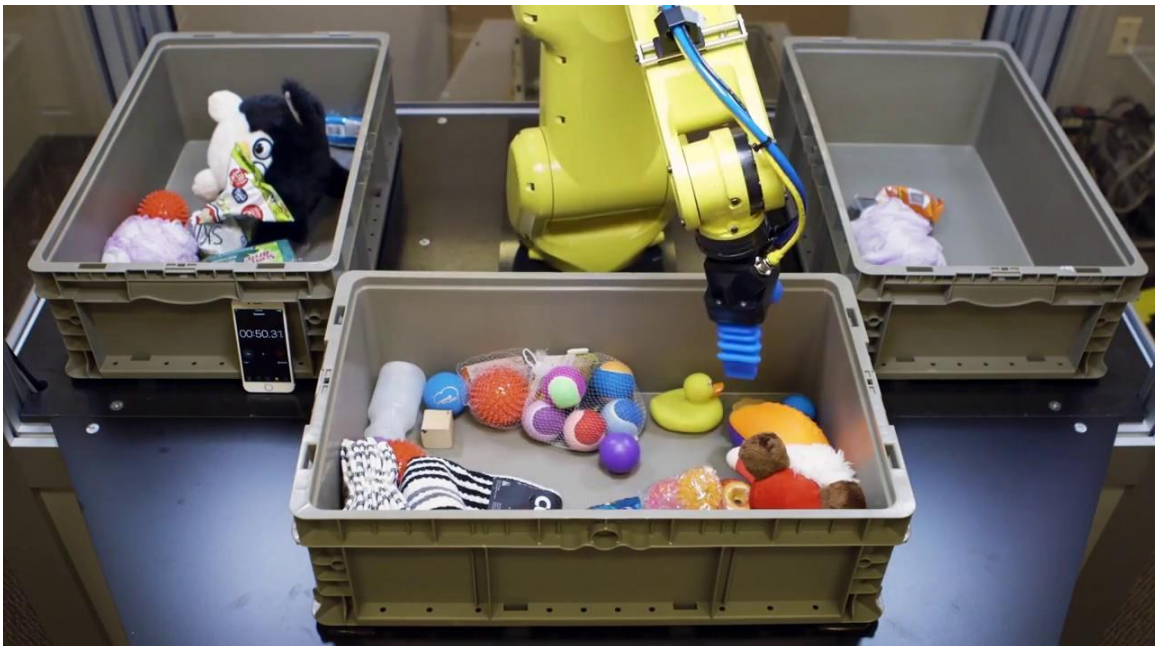

Figure 2 Soft robots in packaging and delivery. Image courtesy softroboticsinc.com [21]

1.3 Aim

In this study we plan to design and test a novel bending actuator mechanism that can be used as one of the grasping mechanisms in soft robots designed mostly for hand rehabilitation [4], [5] but can be applied to other use cases as well. Ours is a hybrid approach combining aspects of the traditional hard robotics with the newer soft robotics. The design incorporates rigid shells to give added support and robustness as well as more precise control. The actuation by pneumatic or fluidic means through a soft elastomer based tube preserves the benefits of soft robots.

CHAPTER 2: LITERATURE REVIEW

2.1 Brief Overview

An actuator is a mechanical component used for control and movement of any mechanism in this case for example used for the movement of individual joints in the fingers of a hand rehabilitation device. They are classified mainly on the basis on the type of movement caused and on the principle on the basis of which they cause the movement, their actuation mechanism.

This review will be restricted to the study of these actuation mechanisms specifically focusing on the mechanism of bending actuators used in soft robotics. We will also shortly discuss the merits and disadvantages of each design. However, we will not delve too much into the various use cases of each design albeit the occasional mention and we will mostly avoid actuators used in hard robotics or in linear actuation cases. At the end we will also compare various soft elastomeric materials used in various designs.

2.2 Pneumatic Networks

Pneumatic networks or pneu-nets consist of a network or series of chambers which are pneumatically actuated. Hence the name pneu-nets. The actuator is made from elastomeric materials. The motion is determined by carefully selecting the wall thickness and the wall or chamber geometry. When the actuator is actuated the less stiff geometry and thinner walls will stretch easily. The same can be done by using different materials having different stiffness. These have been studied and employed by [2][4][5][10][6].

The bending occurs by the "**differential strain effect**". This is an important principle of this field and is therefore explained in detail below.

The chambers expand easily and hence the length of the top part increases. The expansion of the bottom part is constrained using a "strain limiting layer". Thus due to the differential strain of the top and bottom layers the actuator bends into a circular shape.

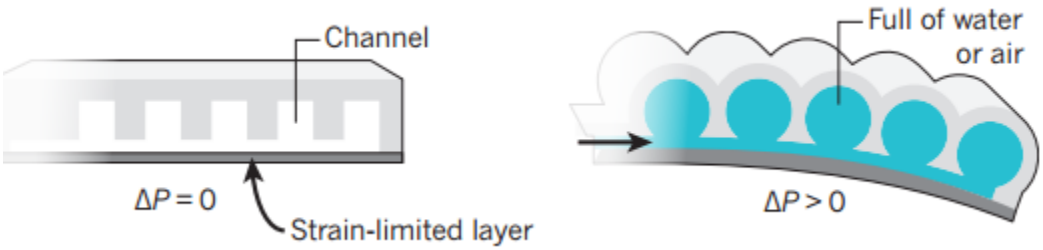

Figure 3 working of a PneuNet [2]

Pneumatic networks require low actuation pressures and are capable of very large bending angles at these low actuation pressure. But pneu-nets are liable to bursting and cannot handle very high pressures. This limits their force output and makes them incapable of creating large forces.

2.2.1 Differential strain Effect

According to this effect when two layers of a body have different lengths the body will deform itself into a circular shape to incorporate the two lengths. As the length or circumference = 2 π r, the outer circumference is larger than the inner circumference hence the circular shape is achieved.

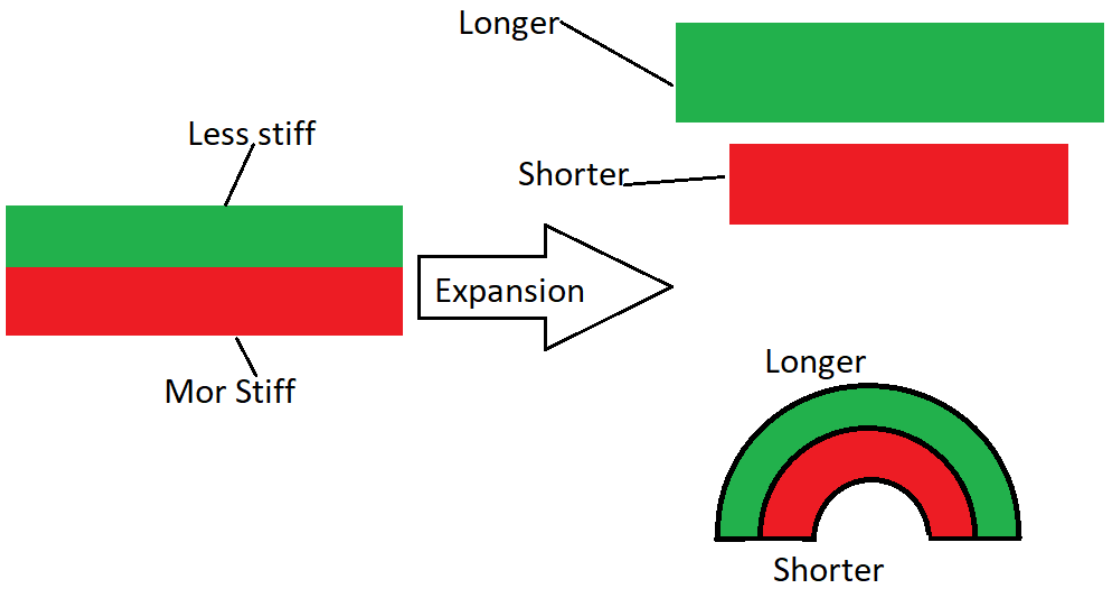

Figure 4 The Differential strain principle

2.3 Fiber reinforced Bending Actuators

These also function on the principle of the differential strain effect. It consists of a chamber made from elastomers. The radial expansion of the chamber is constrained by threads or fibers, these windings force the chamber to expand only in the axial direction. The bottom part of the actuator contains the strain limiting layer which constrains the expansion of the bottom part thus creating a differential strain [12][13][14]. Nordin et al. [11] did not use a strain limiting layer, instead they changed the fiber angles so that the bottom part had tighter windings than the upper part. This also created a differential strain.

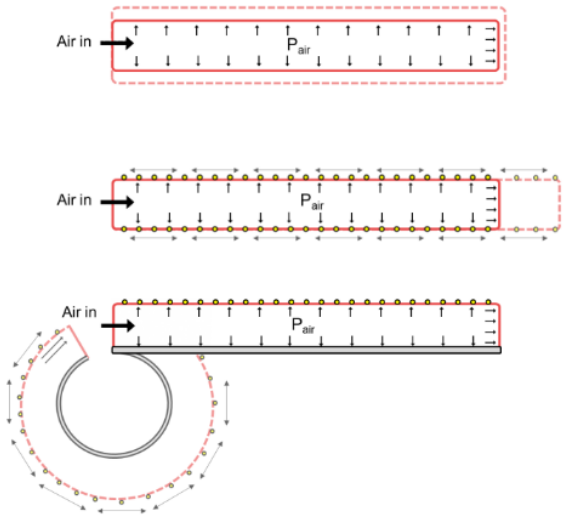

Figure 5 image courtesy soft robotics toolkit [18]

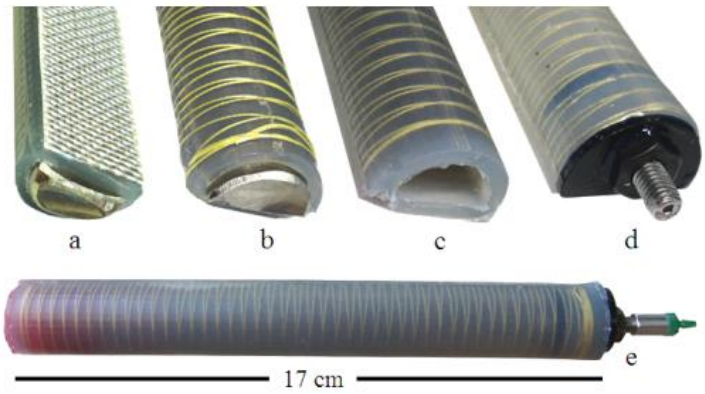

Figure 6 Fiber reinforced bending actuator [13]

2.4 Parallel Combination of Expanding and Contracting Pneumatic Actuators

Bending can be achieved by the parallel combination of expanding pneumatic actuators with contracting actuators, [15][16][19]. This also creates a situation similar to the differential strain effect with the top and bottom layers having different lengths.

Figure 7 Parallel Combination of linear pneumatic actuators to create a bending actuator [15]

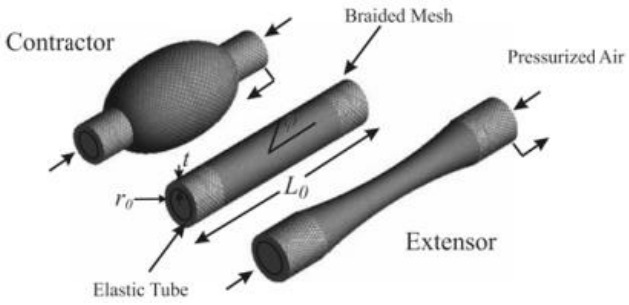

Figure 8 linear actuators [19]

2.5 Manipulating bending geometries and bend control radius

Methods to produce more complicated motions have been explored by recent researchers. Simple bending although very useful limits the uses of soft bending actuators. To get more out of these actuators they need to be made capable of more complex and better controlled motions.

2.5.1 Manipulating the Helix

Connolly et al. manipulated the helix of the windings at different portions of the actuator to produce more complicated motions. By simply varying the fiber angle the researchers were able to tune the actuators to achieve a wide range of motions, including axial extension, radial expansion, and twisting. These motions can be achieved by:

- **Twisting:** By making the fiber windings non-symmetric the actuator will expand in certain direction and will be constrained in certain directions.
- **Axial Extension:** Symmetric windings which completely constrain radial expansion will force the actuator to extend in the axial direction only.
- **Radial Expansion:** A loose symmetric mesh will allow for radial expansion.

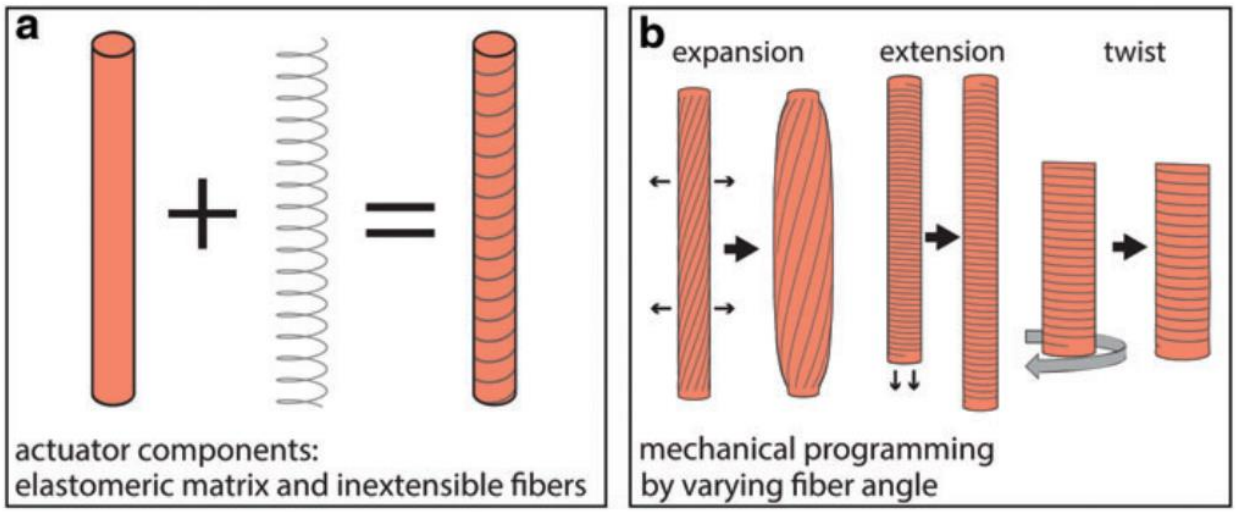

Figure 9 Helix manipulation for complex geometries [17]

2.5.2 Constraining Bending

By constraining the bending at certain portion, it is possible to attain more complex geometries as compared to simple circular bending. Galloway et al. [13] employed sleeves and rigid layers to constrain the bending at certain portions. This caused the actuator to behave as if it consists of rigid links. Yap, Hong Kai, et al. [14] used a similar technique to preprogram the actuator so that it conforms to a desired geometry which in this case is the human hand.

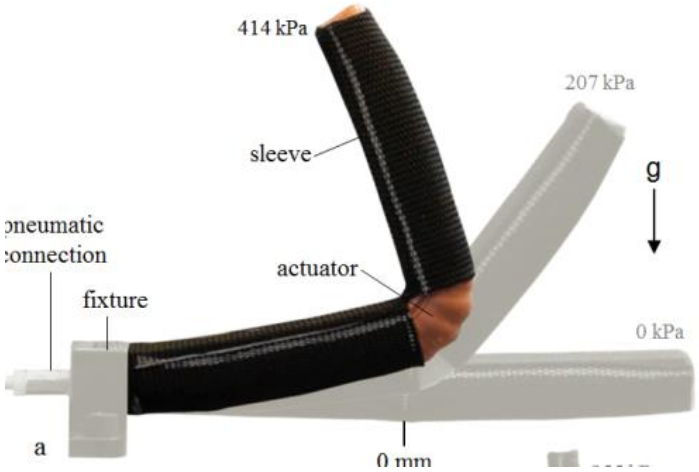

Figure 10 Use of Sleeves [13]

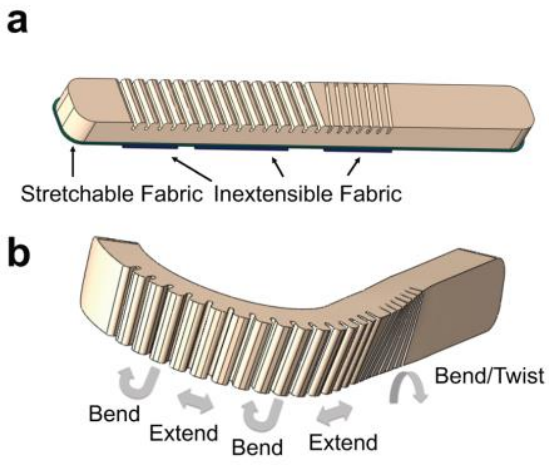

Figure 11 Rigid elements and cuts for shape conformability [14]

2.6 Programmable Hybrid Actuators

Yaohui Chen et al. [3] created a programmable hybrid actuator combining soft and hard components. The actuator consists of a number of shells which can be interlocked allowing the actuator to conform to a variety of shapes.

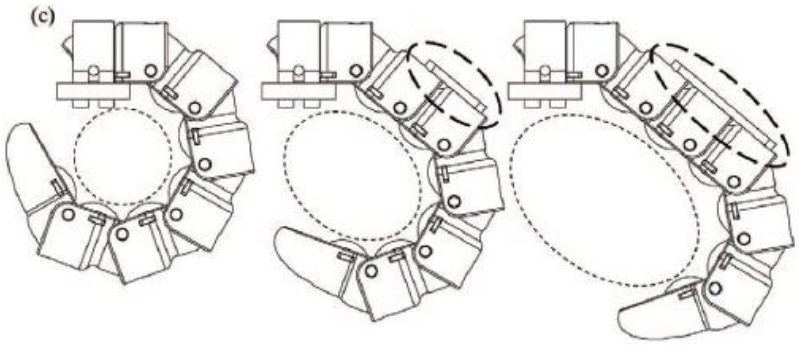

Figure 12 programmable hybrid actuator [3]

2.7 Applications

In the following paragraphs application specific designs are discussed instead of just novel designs applicable to different fields.

2.7.1 Soft Exo Gloves

The concept of soft robotics has been applied to create robotic exo-skeleton gloves especially for rehabilitation and assistance for activities of daily living or ADL.

Yap, Hong Kai, et al. [14] designed a fabric regulated glove which employed rigid elements and cuts to program the actuators.

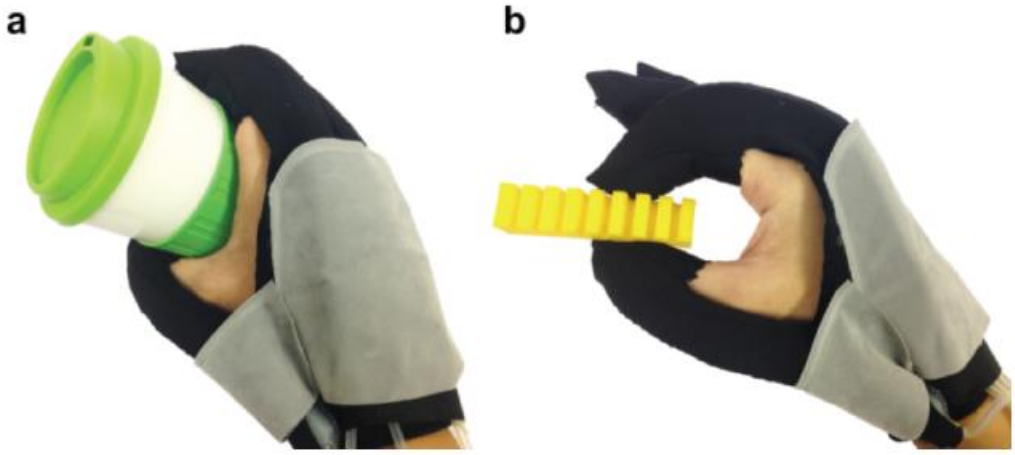

Figure 13 glove made by Yap, Hong Kai, et al [14]

Polygerinos, Panagiotis, et al. [4] created a glove for similar applications using pneu-nets.

Figure 14 soft glove [4]

These gloves are good for rehab and assistance of disabled individuals due to their inherent properties such as:

- **Slow response time:** Due to the nature of the materials and the actuation principles the glove creates motion at a slow rate which complies with the safe limits of human motion.
- **Low Forces:** The activities with daily living generally require a grasping force of no more 7N. The bending actuators are designed to provide forces along these lines even with very high pressures and are thus safer than traditional robotic gloves.

2.7.2 Bio Mimetic Robots

OctArm Robot

McMahan, William, et al. [19] applied the concepts discussed above to create and octopus arm. He employed the use of a parallel combination of linear actuators to create bending actuators. Thanks to the robust McKibben muscles making up the actuators the OctArm is capable of very high grasping forces.

Figure 15 Oct arm made by parallel linear actuators [19]

Manta Swimming Robot

Suzumori, Koichi, et al. [7] used soft bending actuators to create a manta ray robot. The fins of the manta ray were operated through the bending action of the actuators. The body of the manta ray was composed of elastomers similar to the ones used in the actuator.

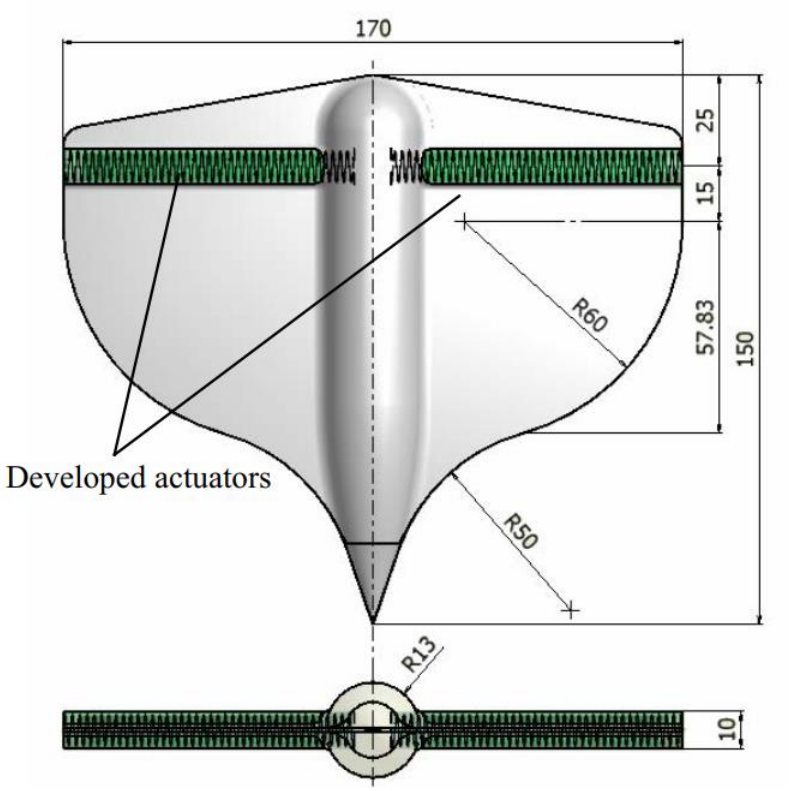

Figure 16 manta swimming robot using soft actuators [7]

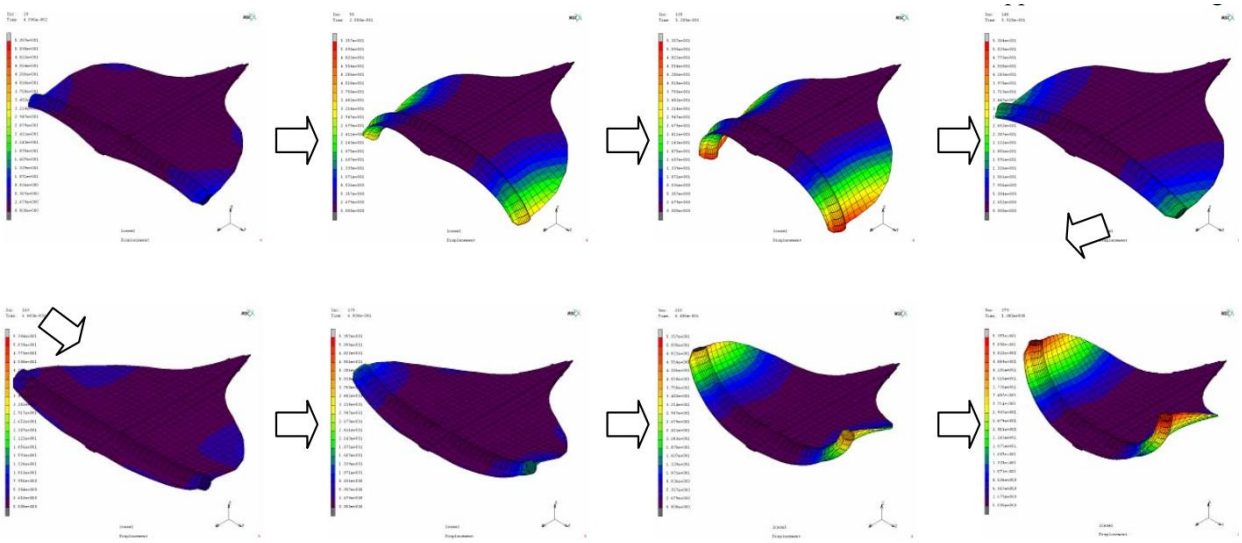

Figure 17 Motions of the manta swimming robot achieved using bending actuators

CHAPTER 3: METHODOLOGY

3.1 Working

The current model consists of a series of shells enclosing a soft inner tube. The shells act as levers which are operated by the expansion of the tube. The levers act to convert the expansion of the tube in to a rotary motion.

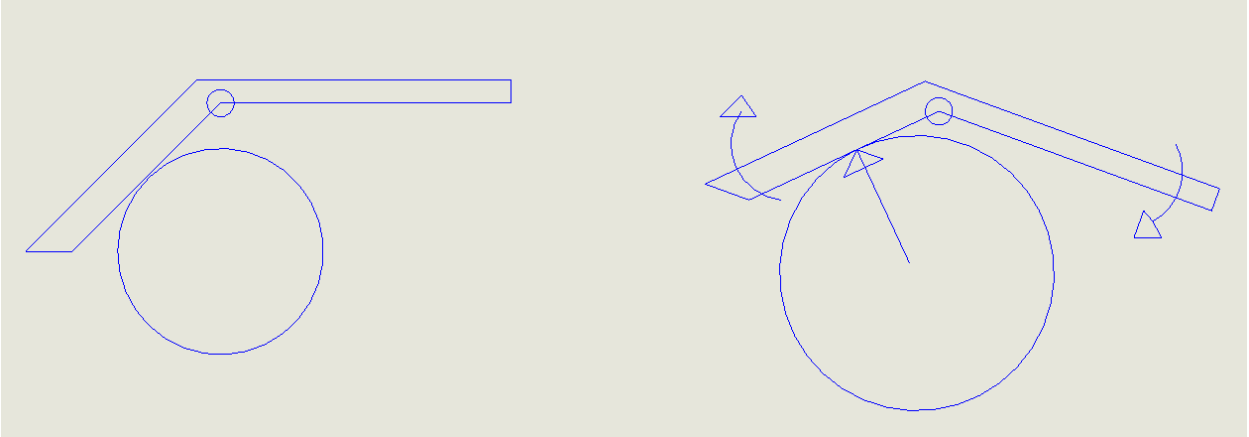

Figure 18 Basic Concept

As a series the rotation angles add up and a circular bend can be attained.

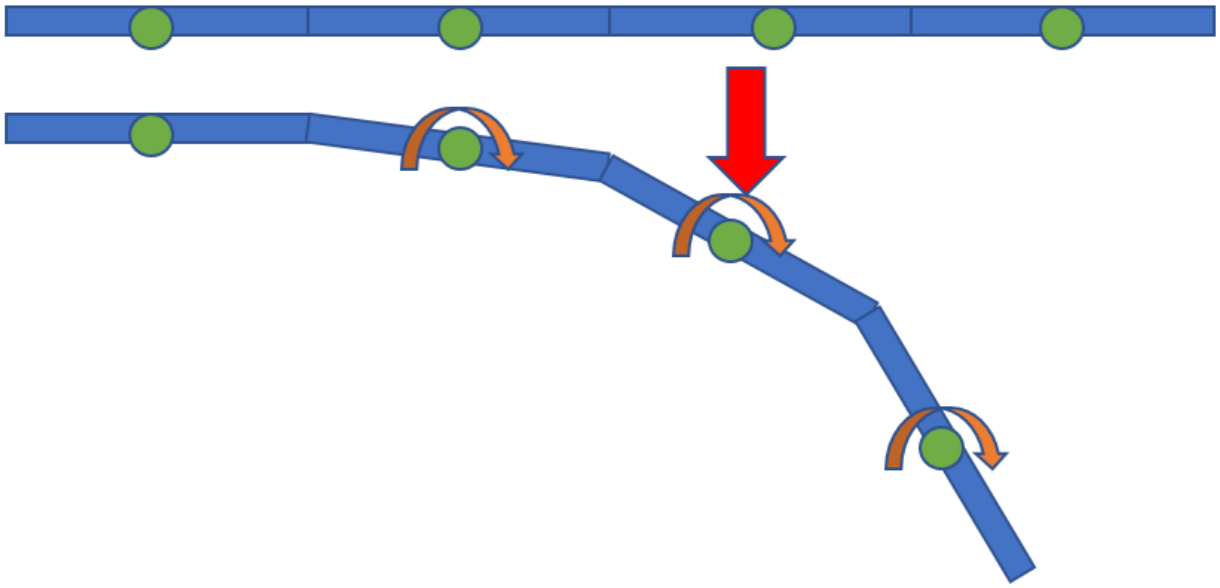

Figure 19 Basic Concept: Network of levers

3.2 Choice of shape

To determine the shape of the tube we went by the approach outlined by Polygerinos et al. [12]. Three cross-sectional shapes were compared to identify the most effective shape for a soft bending actuator. The deciding criteria was which shape requires the least pressure to bend to the same angle while preserving its original cross-sectional shape.

The three shapes were:

1. Hemi circular
2. Circular
3. Rectangular

The dimensions for each shape were obtained using the same cross-sectional area. Assuming a wall thickness of t = a/4, with an input air pressure of P_{in}, the bending torques

(M_a) of internal air pressure against the distal cap of the actuator geometry were calculated as

$$M_a^r = \frac{0.5\ a^3\ P_{in}}{v}$$

$$M_a^{hc} = 0.34\ a^3\ P_{in}$$

$$M_a^c = 0.72\ a^3\ P_{in}$$

The higher value of M_a indicates that the actuator is difficult to bend. Hence the most suitable shape is hemi circular which is what we have used.

3.3 CAD Model

The CAD model was developed using SolidWorks. The model consists of an inner tube covered with shells. For us the model is an iterative process. As we test each design and find out the flaws we improve the design. As of yet we are already on the fourth or fifth iteration. Some of the features that have needed constant tinkering and changing are labelled in the diagrams displayed in this section. Whenever failure occurs in the FEM analysis or the design doesn't work as well as it should we try to find out the reason behind it and work towards changing the design.

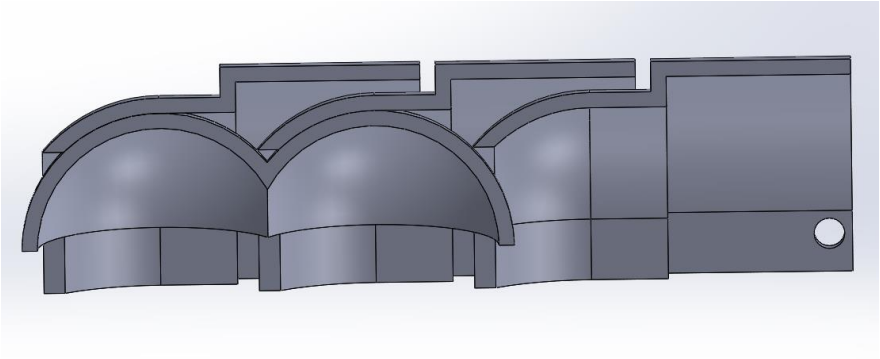

Figure 20 Sectioned view of the assembly

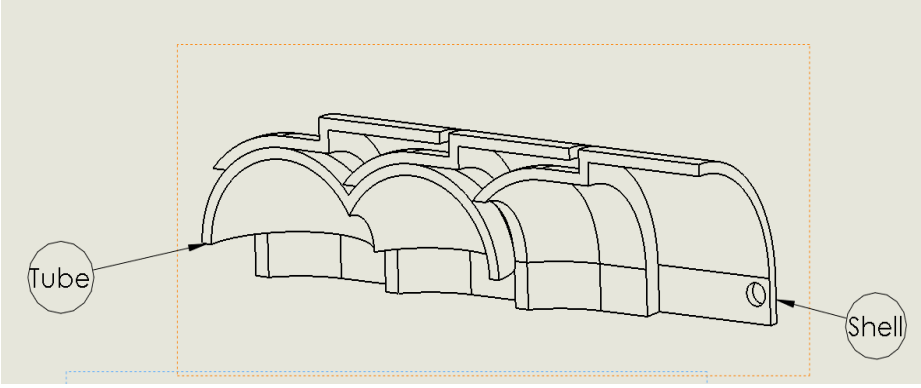

Figure 21 main components of the design

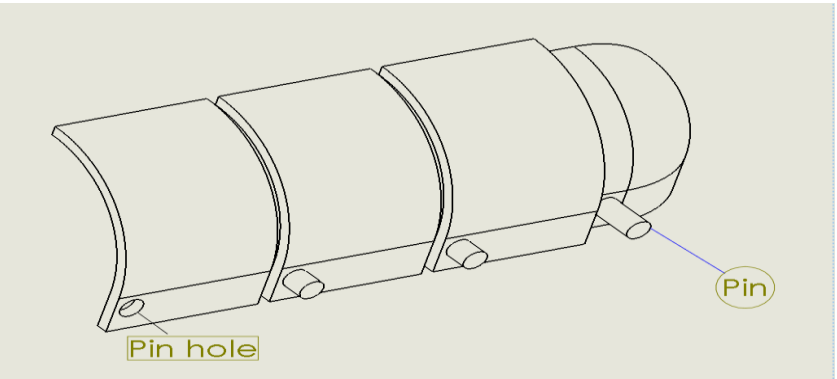

Figure 22 Main components and features of the design

3.4 Modeling of the Actuator

In hard robotics, well-defined analytical models are available which can be referenced to solve any mechanism of mechanical links and the resultant forces they produce. In the case of soft robotics specifically soft actuators, detailed FEM Models are required to account for the hyper-elastic nature. Analytical Models are also available but certain assumptions have to be made to solve the system using them. In this study using these techniques we have tried to obtain a relationship between joint angle and the displacements as well as the relationship between the joint angles and joint forces and torques.

3.4.1 Analytical Modeling

To solve the system analytically, we have to divide the system into two parts, the rigid part and the soft elastomeric part. We then solve the two systems on their own and then integrate the solution at the end. It must be noted that the system itself has been solved generally

using assumptions of linear elasticity due to which factor of error might be present. However, this can be accounted for later using the real-world experiment Model.

3.4.1.1 Model for Rigid Links

Our current iteration of the design consists of six rigid shells connected to each other in a train type of alignment back to back using pins. They can be assumed as rigid links if the effective length link **L** is assumed as the distance between the pins and q_1-q_6 as the joint angles for the each of the shells as shown in Figure

Using the Denavit-Hartenberg notation we can define the fixed link parameters and joint variable as given in Table, more commonly known as dh parameters for each of the joints.

I	α_{i-1}	a_{i-1}	d_i	θ_i
1	0	L	0	q_1
2	0	L	0	q_2
3	0	L	0	q_3
4	0	L	0	q_4
5	0	L	0	q_5
6	0	L	0	q_6

Table 1 Denavit-Hartenberg (DH) parameter

The complete pose of the end-effector can be defined as follows

$$E = R_z(q_1)T_x(L)R_z(q_2)T_x(L)R_z(q_3)T_x(L)R_z(q_4)T_x(L)R_z(q_5)T_x(L)R_z(q_6)T_x(L) \quad (1)$$

This is equivalent to six individual transformations relative to each of joint up until the end-effector where

$$E = {}^{0}_{6}T = {}^{0}_{1}T\,{}^{1}_{2}T\,{}^{2}_{3}T\,{}^{3}_{4}T\,{}^{4}_{5}T\,{}^{5}_{6}T \tag{2}$$

These transformations relate each joint frame with the next in the alignment and when compounded together represent the transformation of the end effector frame to the base frame. Here each individual transformation matrix can be defined as follows

$${}^{0}_{1}T = \begin{bmatrix} \cos q_1 & -\sin q_1 & 0 & L \\ \sin q_1 & \cos q_1 & 0 & 0 \\ 0 & 0 & 1 & 0 \\ 0 & 0 & 0 & 1 \end{bmatrix}$$

$${}^{1}_{2}T = \begin{bmatrix} \cos q_2 & -\sin q_2 & 0 & L \\ \sin q_2 & \cos q_2 & 0 & 0 \\ 0 & 0 & 1 & 0 \\ 0 & 0 & 0 & 1 \end{bmatrix}$$

$${}^{2}_{3}T = \begin{bmatrix} \cos q_3 & -\sin q_3 & 0 & L \\ \sin q_3 & \cos q_3 & 0 & 0 \\ 0 & 0 & 1 & 0 \\ 0 & 0 & 0 & 1 \end{bmatrix}$$

$${}^{3}_{4}T = \begin{bmatrix} \cos q_4 & -\sin q_4 & 0 & L \\ \sin q_4 & \cos q_4 & 0 & 0 \\ 0 & 0 & 1 & 0 \\ 0 & 0 & 0 & 1 \end{bmatrix}$$

$${}^{4}_{5}T = \begin{bmatrix} \cos q_5 & -\sin q_5 & 0 & L \\ \sin q_5 & \cos q_5 & 0 & 0 \\ 0 & 0 & 1 & 0 \\ 0 & 0 & 0 & 1 \end{bmatrix}$$

$$ {}^{5}_{6}T = \begin{bmatrix} \cos q_6 & -\sin q_6 & 0 & L \\ \sin q_6 & \cos q_6 & 0 & 0 \\ 0 & 0 & 1 & 0 \\ 0 & 0 & 0 & 1 \end{bmatrix} $$

Where the final can be inferred as

$$ E = \begin{bmatrix} r_{11} & r_{12} & r_{13} & r_{14} \\ r_{21} & r_{22} & r_{23} & r_{24} \\ r_{31} & r_{32} & r_{33} & r_{34} \\ r_{41} & r_{42} & r_{43} & r_{44} \end{bmatrix} \quad (3) $$

Since we only require only the position of the end effector, it can be directly inferred from the pose as the translations in the x-y plane where

$$ \begin{bmatrix} x \\ y \end{bmatrix} = \begin{bmatrix} r_{14} \\ r_{24} \end{bmatrix} \quad (4) $$

As the system has six degrees of freedom the analytical solution becomes too complex to evaluate so in such cases we utilize the trchain2 command in Matlab robotics toolbox we numerically evaluate r_{14} and r_{24} which are the end effector coordinates. They are entirely dependent upon the joint variables q_1-q_6 and the link length L which is a known constant.

3.4.1.2 Model for Soft-Expanding Elastomer

In order to solve the non-linear elastomeric system we will consider a hemispherical elastomeric tube element pinned at one end and free at the other as shown in Figure1[12]. To consider this assumption within our model we will have to divide the elastomer tube into per shell segments. Also initially our actual model is a hemi sphere tube with circular indentations in the hemispherical portion. Upon pressurizing, it comes into contact with the shell surface and after complete contact we assume it forms a near uniform

hemispherical surface and becomes restricted by the shell from expanding in the circumferential direction after initial contact and becomes similar to soft fiber reinforced bending actuator [12].

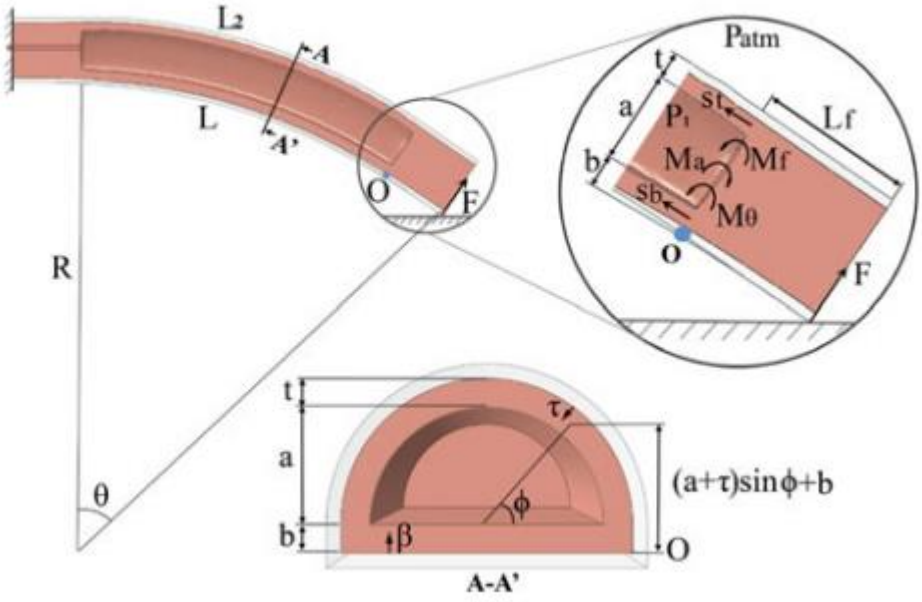

Figure 23 Side view of the expanding tube element in a bending state. Close-up view: view of the end fulcrum showing the generated moments. Lower center: Cross-sectional view of the tube element with local coordinates.

3.4.1.3 Material Model

As the elastomeric tube as fabricated using silicone rubber, and the material shows hyper elastic behavior during its expansion we have to model it as an incompressible Neo-Hookean material [20]. Now we assume the strain energy as

$$W = \frac{\mu}{2}(I_1 - 3) \quad (5)$$

Here I_1 is an invariant (remains constant) of the various stretch ratios λ_1, λ_2 and λ_3 in the axial, circumferential and radial directions and so is defined by the equation

$$I_1 = \lambda_1^2 + \lambda_2^2 + \lambda_3^2 \quad (6)$$

In (5) μ represents the shear modulus of the given material. The general form of the principal normal stresses can thus be obtained as

$$s_i = \frac{\partial W}{\partial \lambda_i} - \frac{P}{\lambda_i} \quad (7)$$

The above equation is a function of strain energy W, stretch ratio λ_i and a Lagrange Multiplier P.

3.4.1.4 Model for Bending Forces and Torques

A model was developed to find the Moments and contact forces produced within the elastomeric system in terms of input pressure and joint angle in free space while comparing the system to a soft fiber reinforced model [12]. We assume that when compressed air at pressure $P_{in}$is provided at one end of the system then then considering one link, a lever force will be generated causing the link to bend in the clockwise direction by an angle θ which can be considered as the join variable of the individual link and *R* the vertical distance of the tube from the pinned joint. Similar to the fiber reinforced system [12] the shell acts as a hard constraint to the expanding tube. Here we ignore the dynamics related to the pressurization of the tube and always assume a uniform bending curvature.

In (6) λ_1 was given as the axial stretch ratio, since the material was constrained in expanding in the circumferential direction, the expansion in this direction was assumed to be negligible thus $\lambda_2 = 1$. Now using the incompressibility equation (8) we can obtain (9)

$$\lambda_1\lambda_2\lambda_3 = 1 \tag{8}$$

$$\lambda_1 = \lambda, \lambda_2 = 1, \lambda_3 = \frac{1}{\lambda} \tag{9}$$

Here λ_3 is the stretch in the radial direction. Now if it is assumed that a vanishing stress occurs in the radial direction (10) then by combing (7) with (6) and (5) we can obtain

$$s_1 = \frac{\partial W}{\partial \lambda_1} - \frac{P}{\lambda_1} = \mu\left(1 - \frac{1}{\lambda^3}\right) \tag{10}$$

$$s_2 = \frac{\partial W}{\partial \lambda_2} - \frac{P}{\lambda_2} = \mu\left(1 - \frac{1}{\lambda^2}\right) \tag{11}$$

$$s_3 = \frac{\partial W}{\partial \lambda_3} - \frac{P}{\lambda_3} = 0 \tag{12}$$

$$P = \mu\lambda_3^2 = \frac{\mu}{\lambda^2} \tag{13}$$

For the working range of $1 \leq \lambda < 1.5$, it was found that the circumferential stress s_2 was many times smaller than s_1. Thus only s_2 was assumed as the only non-vanishing principal stress denoted by *S*.

Using Figure 1 we can see that about the fulcrum O, moment equilibrium [12] is established, due to the material internally stretching, which is given by

$$M_a = M_\theta \tag{14}$$

However, this is the case where the free end of the bending actuator is not in contact with anything so there is no contact Torque generated. M_a is the moment caused by the internal air pressure and $M_\theta$is the combined moment of the internal stretch stresses s_b and s_t on each of the bottom and top layers. As the geometry was assumed as hemispherical, the moment can thus be calculated [12] by

$$M_a = \frac{4a^3+3\pi a^2 b}{6}(P_{in}) \tag{15}$$

However, in the case of contact as shown in Figure 1 (14) becomes

$$M_a = M_\theta + M_f \tag{16}$$

Where $M_f = FL_f$ is the contact moment, L_f is the moment arm and F is the contact force. This however can be adjusted in the case of a contact patch to find pressure. Now if we combine the effect of stresses acting on the top and bottom layers, the acting torque becomes.

$$M_\theta = \int_0^b s_\beta \,.\, 2(a+t)L\beta d\beta + 2\int_0^t \left(\int_0^{\frac{\pi}{2}} s_{\tau,\varphi}\left((a+\tau)^2 \sin\varphi + b(a+\tau)\right)Ld\varphi\right)d\tau \tag{17}$$

To construct the above equation we have had introduce the local coordinates β and τ, for the bottom and top layer respectively (Figure1). Now the longitudinal stretch and the strain can be calculated as

$$\lambda_\beta = \frac{R+\beta}{R} = \frac{\frac{L}{\theta}+\beta}{L/\theta} = \frac{\beta\theta}{L} + 1 \tag{18}$$

$$s_\beta = \mu\left(\lambda_\beta - \frac{1}{\lambda^3{}_\beta}\right) \tag{19}$$

$$\lambda_{\tau,\varphi} = \frac{R+b+\sin\varphi(a+\tau)}{R} \tag{20}$$

$$s_{\tau,\varphi} = \mu\left(\lambda_{\tau,\varphi} - \frac{1}{\lambda^3{}_{\tau,\varphi}}\right) \tag{21}$$

By substituting (18) to (21) into (14) we can simplify the equation by eliminating s and λ, and it becomes possible to elaborate that M_θ is a function of just μ ,a ,b ,t and θ. However, again due to its complexity the integral in (17) cannot be solved analytically but can be solved numerically since the rest are material or geometric constants and can be determined through testing, whereas θ i.e bending angle is the only variable. Hence the contact force and torques can be determined.

3.4.1.5 Model for Complete Mechanism

Up until now we have modeled system using individual link segments and so displacements for link can be generated using the relevant transformations. Similarly, we have modeled the system of a single soft bending actuator. However, it is possible to extrapolate it to our complete system with any number of links by just substituting the bending angle θ by the individual joint angles q_1-q_6. Thus our system becomes a train of individual shell links each with its own pinned elastomeric bending actuator which can be modeled as soft restricted bending actuators dependent upon the joint variables.

Thus we have now modeled a system that is flexible enough to account for any number of links, and if the pressure, material and geometric properties are known then the displacements, forces and moments become dependent only upon the joint angles.

3.4.2 Material Selection

After meticulous searching the following 5 materials were found as suitable candidates to be used for the hyper-elastic tube. Ecoflex was too soft, while dragon-skin required more actuation pressure. Elastoil M4601 from Wacker chemical was a good fit but due to unavailability, HY-625 RTV was used for the initial prototyping for the following reasons:

- It had greater shore hardness. As our material was interacting with rigid shells, this silicone provided good fluidity with moderate hardness.
- It had half the curing time.
- It was locally available and cheap.
- It had relatively high tear strength as compared to the silicones provided by Smooth-On, Inc.

Materials	Dragon Skin 10	Elastoil M4601	Elastoil M4601 28A	EcoFlex 00-30	HY-625 RTV-2
Supplier	Smooth-On, Inc.	Wacker chemical	Wacker chemical	Smooth-On, Inc.	Almost all across the world
Printers	Mould	ACEO	ACEO	Mould	Has to be moulded

Price	$ 30.5 / 0.91kg	17418.69 for a lattice of 26 mm x 20 mm x 22 mm	17418.69 for a lattice of 26 mm x 20 mm x 22 mm	$ 30.1 / 0.91kg	$20/kg
Location	USA	Germany	Germany	Pakistan	China
Rate from other sources	Same	$76 or 46 Euro	$76 or 46 Euro	-Depends on size relatively affordable	$9
Curing Time	5 hours	12 hours	10 hours	4 hours	4-5 hours

Table 2 Cross comparison of different material candidates

The choice of material was further justified when we performed the analysis using Ecoflex 00-30. As seen in the analysis. As soon as the material comes in contact with the shell, it starts to expand into the free space which leads to an error in ABAQUS. The design requires a material with higher elastic modulus.

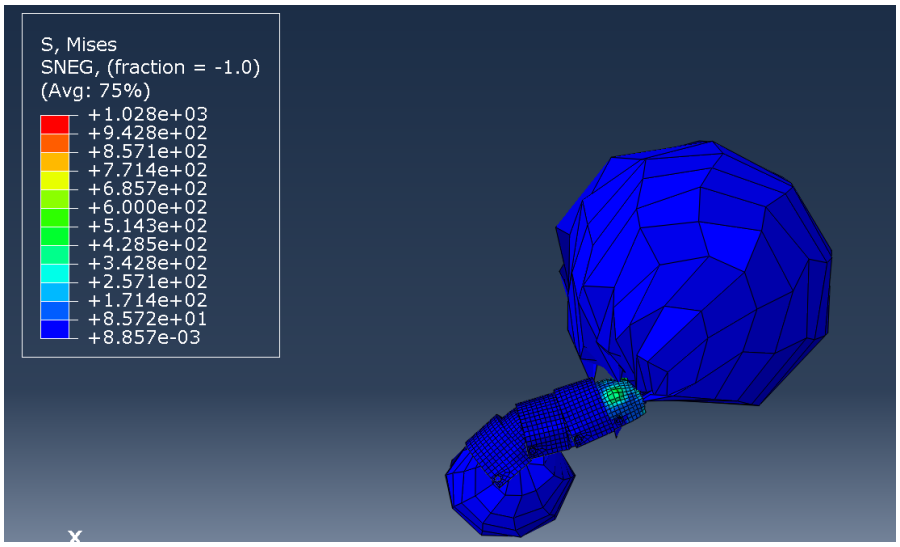

Figure 24 Extreme expansion of ecoflex proving the need for a stiffer material

Below are the detailed properties of the materials that we considered for the project. The properties were obtained from the manufacturers themselves.

Elastosil M4601 by Wacker Chemicals

Typical general characteristics		
Property	**Inspection Method**	**Value**
Elongation at break	ISO 37	700 %
Hardness Shore A	ISO 868	28
Mix ratio at (pbw)	A : B	9 : 1
Tensile strength	ISO 37	6.5 N/mm²
Viscosity at 23 °C, after stirring	ISO 3219	15000 mPa s
Viscosity at 23 °C, after stirring	ISO 3219	800 mPa s
Viscosity at 23 °C	ISO 3219	10000 mPa s
Density at 23 °C		1.01 g/cm³
Density at 23 °C in water	ISO 2781	1.13 g/cm³
Density at 23 °C		1.14 g/cm³
tear-strength	ASTM D 624 B	> 30 N/mm

Figure 25 properties of elastosil M4601

Dragon Skin by Smooth On Inc.

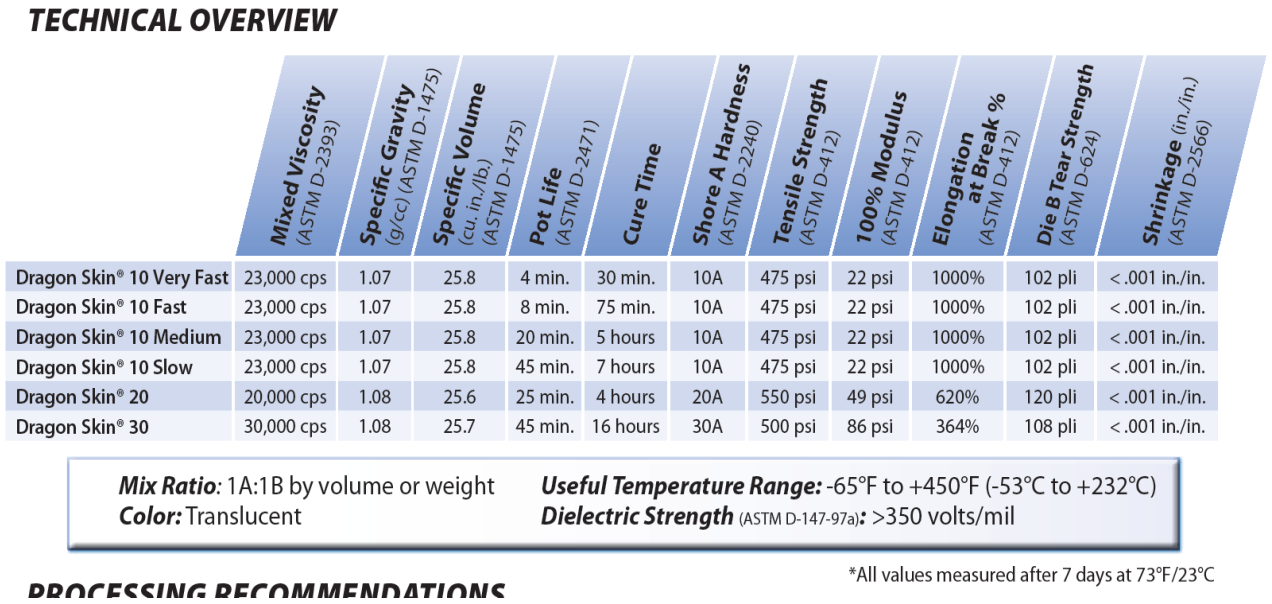

TECHNICAL OVERVIEW

	Mixed Viscosity (ASTM D-2393)	Specific Gravity (g/cc) (ASTM D-1475)	Specific Volume (cu. in./lb.) (ASTM D-1475)	Pot Life (ASTM D-2471)	Cure Time	Shore A Hardness (ASTM D-2240)	Tensile Strength (ASTM D-412)	100% Modulus (ASTM D-412)	Elongation at Break % (ASTM D-412)	Die B Tear Strength (ASTM D-624)	Shrinkage (in./in.) (ASTM D-2566)
Dragon Skin® 10 Very Fast	23,000 cps	1.07	25.8	4 min.	30 min.	10A	475 psi	22 psi	1000%	102 pli	< .001 in./in.
Dragon Skin® 10 Fast	23,000 cps	1.07	25.8	8 min.	75 min.	10A	475 psi	22 psi	1000%	102 pli	< .001 in./in.
Dragon Skin® 10 Medium	23,000 cps	1.07	25.8	20 min.	5 hours	10A	475 psi	22 psi	1000%	102 pli	< .001 in./in.
Dragon Skin® 10 Slow	23,000 cps	1.07	25.8	45 min.	7 hours	10A	475 psi	22 psi	1000%	102 pli	< .001 in./in.
Dragon Skin® 20	20,000 cps	1.08	25.6	25 min.	4 hours	20A	550 psi	49 psi	620%	120 pli	< .001 in./in.
Dragon Skin® 30	30,000 cps	1.08	25.7	45 min.	16 hours	30A	500 psi	86 psi	364%	108 pli	< .001 in./in.

Mix Ratio: 1A:1B by volume or weight
Color: Translucent

Useful Temperature Range: -65°F to +450°F (-53°C to +232°C)
Dielectric Strength (ASTM D-147-97a)**:** >350 volts/mil

*All values measured after 7 days at 73°F/23°C

PROCESSING RECOMMENDATIONS

Figure 26 Properties of dragon skin

Ecoflex 00-30 by Smooth On Inc.

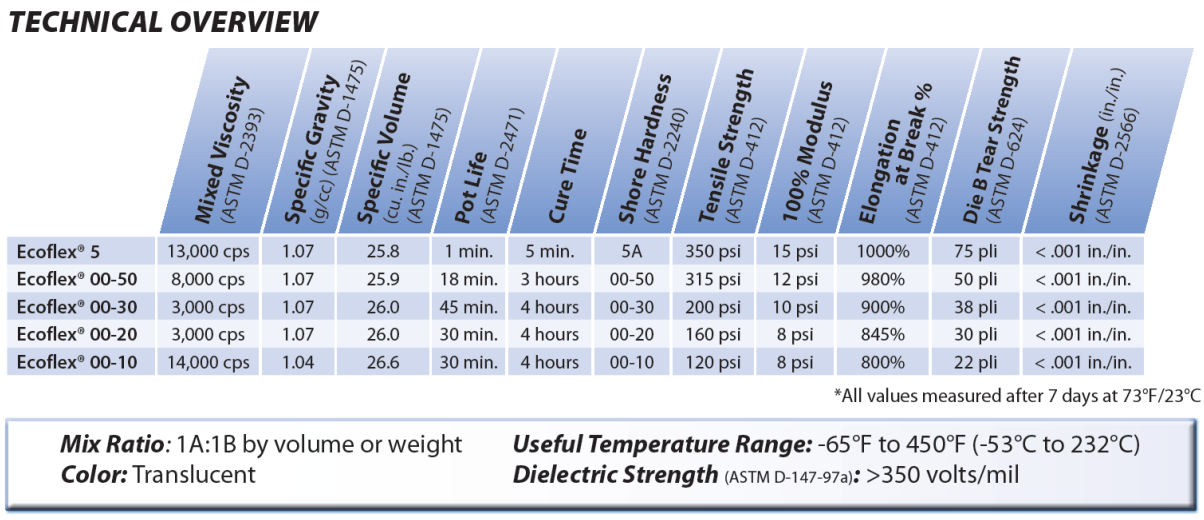

TECHNICAL OVERVIEW

	Mixed Viscosity (ASTM D-2393)	Specific Gravity (g/cc) (ASTM D-1475)	Specific Volume (cu. in./lb.) (ASTM D-1475)	Pot Life (ASTM D-2471)	Cure Time	Shore Hardness (ASTM D-2240)	Tensile Strength (ASTM D-412)	100% Modulus (ASTM D-412)	Elongation at Break % (ASTM D-412)	Die B Tear Strength (ASTM D-624)	Shrinkage (in./in.) (ASTM D-2566)
Ecoflex® 5	13,000 cps	1.07	25.8	1 min.	5 min.	5A	350 psi	15 psi	1000%	75 pli	< .001 in./in.
Ecoflex® 00-50	8,000 cps	1.07	25.9	18 min.	3 hours	00-50	315 psi	12 psi	980%	50 pli	< .001 in./in.
Ecoflex® 00-30	3,000 cps	1.07	26.0	45 min.	4 hours	00-30	200 psi	10 psi	900%	38 pli	< .001 in./in.
Ecoflex® 00-20	3,000 cps	1.07	26.0	30 min.	4 hours	00-20	160 psi	8 psi	845%	30 pli	< .001 in./in.
Ecoflex® 00-10	14,000 cps	1.04	26.6	30 min.	4 hours	00-10	120 psi	8 psi	800%	22 pli	< .001 in./in.

*All values measured after 7 days at 73°F/23°C

Mix Ratio: 1A:1B by volume or weight
Color: Translucent

Useful Temperature Range: -65°F to 450°F (-53°C to 232°C)
Dielectric Strength (ASTM D-147-97a)**:** >350 volts/mil

Figure 27 Properties of EcoFlex 00-30.

HY-625 by Shenzhen Hong Ye Jie Aerospace New Material Co. Ltd.

Technical Parameters

Model	Color	Mixing ratio (%)	Pot life (mins, under 25℃)	Curing time (hrs,under 25℃)	Hardness (Shore A)	Tensile-strength (MPa)	Tear-strength (kN/m)	Viscosity （After A/B mixed ,mPa.s）	Shrinkage rate (%)	Elongation （%）
HY-625	White	2-3	30-40	4-5	25±2	4.8±0.5	29±2	25000± 5000	≤0.3%	400%

Figure 28 Properties of HY-625

3.4.3 FEM Modelling

The mathematical model gives us an insight into the response of the proposed actuator to the pressure applied to the tube. However, it cannot capture certain aspects of the factors that affect the behavior or our hybrid actuator. Firstly, the assumption that there is no circumferential stress is accounted for in the mathematical model proposed. Secondly, we analyzed both the soft tube and the rigid actuator separately. FEM on the other hand integrates both in while calculating the forces and bending angles. Thirdly, FEM models, provide a slightly pragmatic description of the nonlinear reaction of the actuator at a higher computational cost. Another advantage of using Finite Element Analysis is that the deformation of the hyperplastic material can readily be visualized eventually leading to a

greater understanding of the influence of local strain on global actuator performance. Prior work done on Finite Element Analysis of soft elastomeric actuators has been done but very little amount of work has been done on hybrid actuators and to validate these models.

3.4.3.1 Material Specifications Used

The material chosen was RTV (Room Temperature Vulcanizing) silicone rubber, namely HY-625 imported from China. The Stress-Strain values are to be obtained from the UTS testing. Meanwhile, the material currently being modeled is elastosil M4601 by Wacker Chemicals. Some of the values were approximated from the curves and test results run by Mosadegh, Bobak, et al. [22].Two different models were used. The first was a simple elastic material with Mass Density = 0.00107 g/mm^3, Poisson's ratio = 0.45 and Young's Modulus = 2 MPa. The second was the non-linear Ogden model using coefficients with parameter values N = 3, mu1 =0.001887, alpha1 = -3.848, mu2 = 0.02225, alhpa2 =0.6632, mu3 = 0.003574, alpha3 = 4.225 D1= 2.9259 D2= 0 D3 = 0 and Damping with Alpha = 0.4

The material used for shells was 3D printable ABS, to ensure rapid prototyping and cheap and easy manufacturing. The Density = 0.00105 g/mm^3 = 1050 kg/m^3, Young's Modulus = 20 GPa, Poisson's ratio = 0.3. The shell was designed in Solid works and then imported in ABAQUS Standard/Explicit model.

3.4.3.2 Mesh Details and Specifications

The parts were meshed using Hex-dominated structure as shown. As the geometry was not simplified, define datum planes were defined and the part was cut along the planes to ensure uniform meshing. The soft tube was made using a shell-element in ABAQUS with a thickness of 1.5mm. The element for the shell was “C3D8R”: An 8-node linear brick, reduced integration, hourglass control. For the tube, it is a “S4R”: A 4-node doubly curved thin or thick shell, reduced integration, hourglass control, finite membrane strains. The next step was the section assignments. Both the sections for the rigid shell and the hyper-elastic tube were defined. The parts were assembled such that the pin and holes were co-axial.

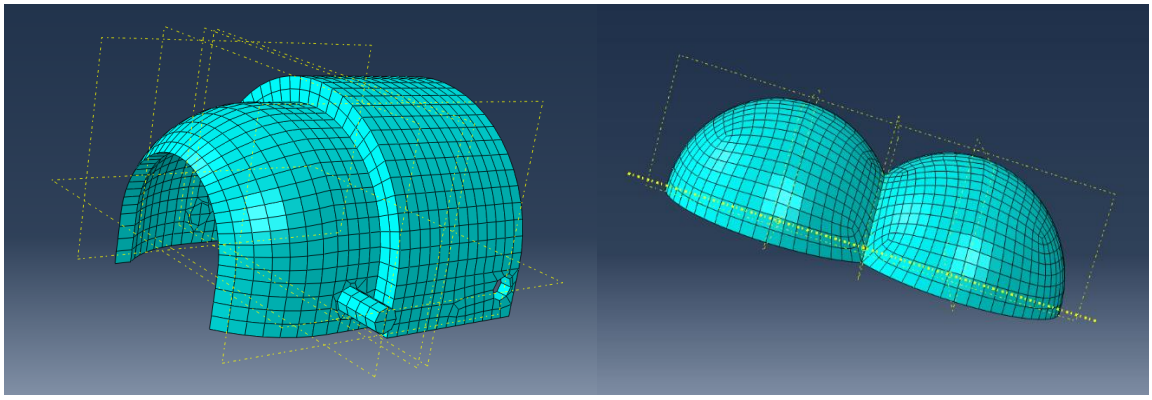

Figure 29 the mesh for the shell (left) and tube (right)

3.4.4 Analysis Details

First the analysis was done for a 3-shell actuator. The shells were assembled as shown. The pin constraint was implemented by coupling a reference point with that particular pin to

make things simple. Hinge connector was also used and it gave the same results. The assembly and the constraint are shown.

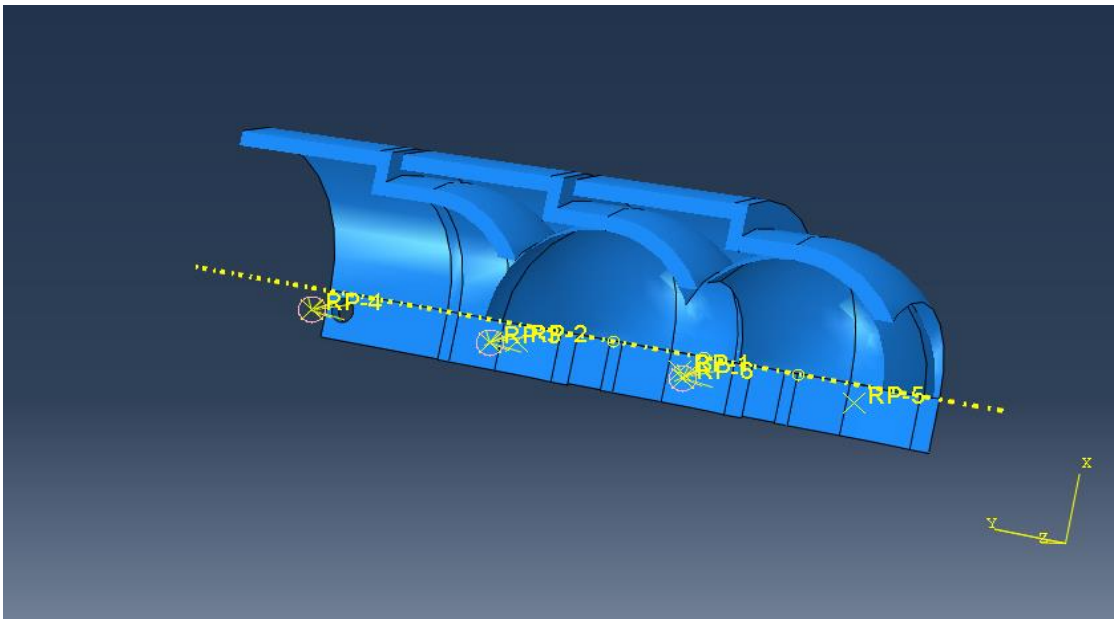

Figure 30 Open view of Model

The outer pin surface and the reference points were coupled using kinematic coupling. This helped us define boundary conditions as we can define the conditions on the reference point rather than the surface. The boundary conditions defined are also shown;

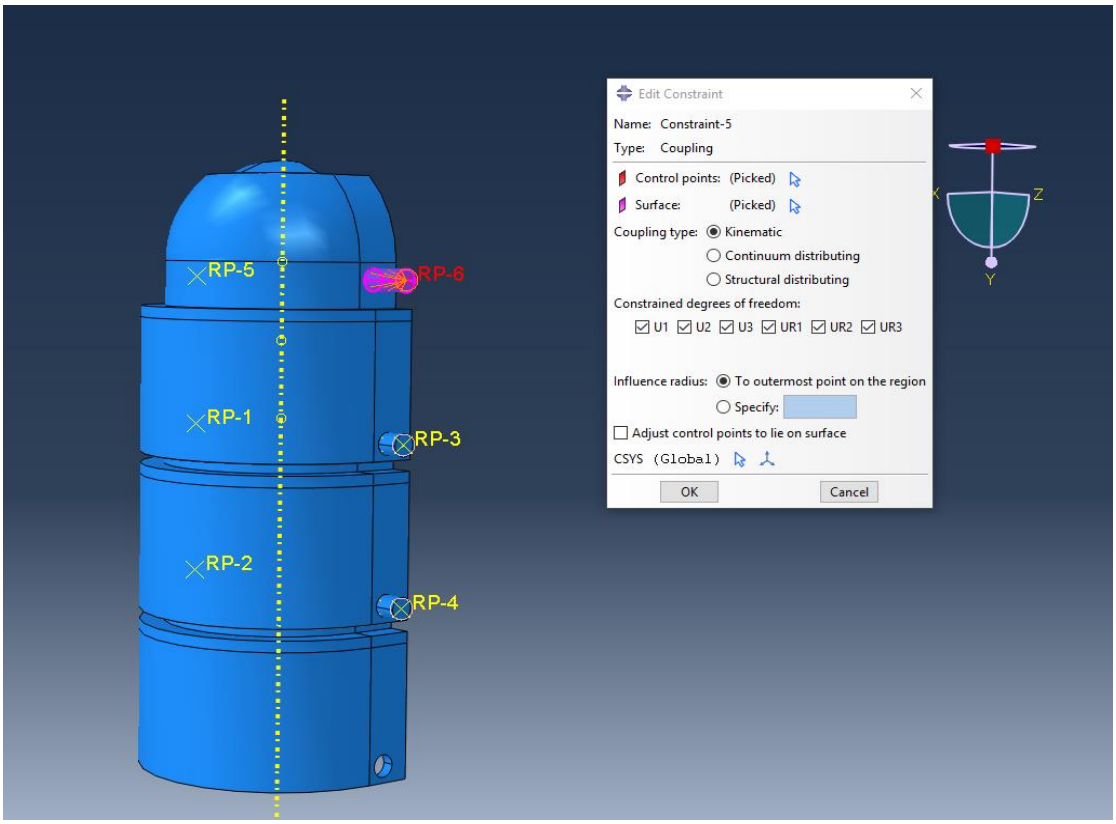

Figure 31 View showing Model Constraint

The shell was encastered from the bottom to ensure that it doesn't displace out of position when pressure is applied. The pins were allowed to move in the X-Y plane and only rotation along the desired plane (i.e.) Z was permitted. Everything was described according to the global coordinate system. Next was the load definitions; the pressure of 150 KPa was applied to the inner side of the shell. Practically, the tube is closed from the bottom but during our analysis the pressure is applied on the desired surface so definition of a bottom plate was deemed unnecessary. The load step defined was a dynamic explicit one because **an explicit dynamic analysis:**

- Is computationally efficient for the analysis of large models with relatively short dynamic response times and for the analysis of extremely discontinuous events or processes;
- Allows for the definition of very general contact conditions
- Uses a consistent, large-deformation theory—models can undergo large rotations and large deformation.
- Can use a geometrically linear deformation theory—strains and rotations are assumed to be small.
- Can be used to perform an adiabatic stress analysis if inelastic dissipation is expected to generate heat in the material.
- Can be used to perform quasi-static analyses with complicated contact conditions; and
- Allows for either automatic or fixed time incrementation to be used—by default, Abaqus/Explicit uses automatic time incrementation with the global time estimator.

The time period was set to 3 seconds and the NLGEOM was turned on to account for geometric nonlinearity of the system.

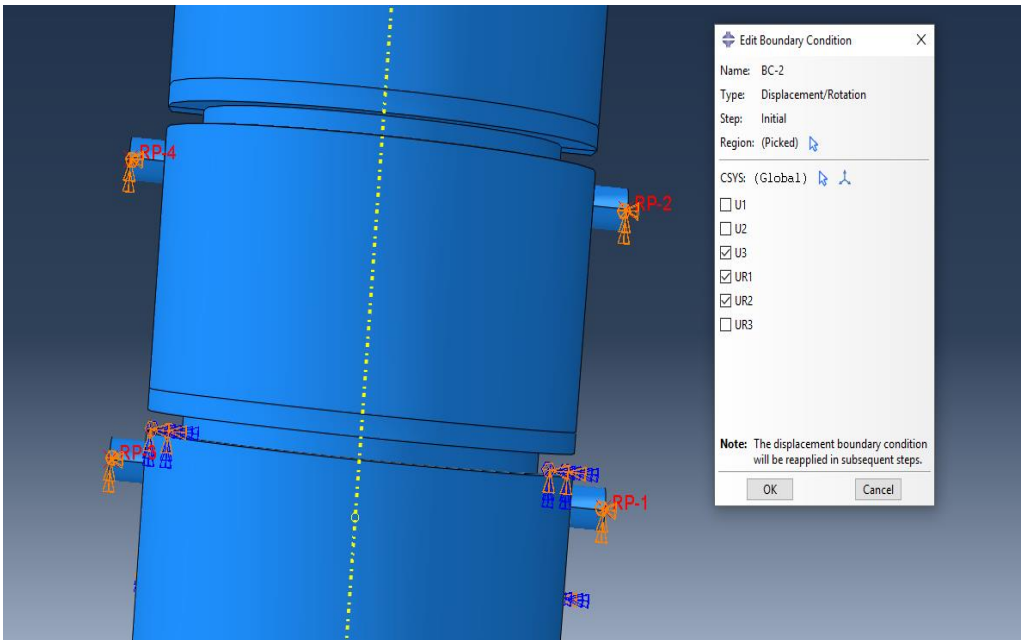

Figure 32 View showing possible movement directions

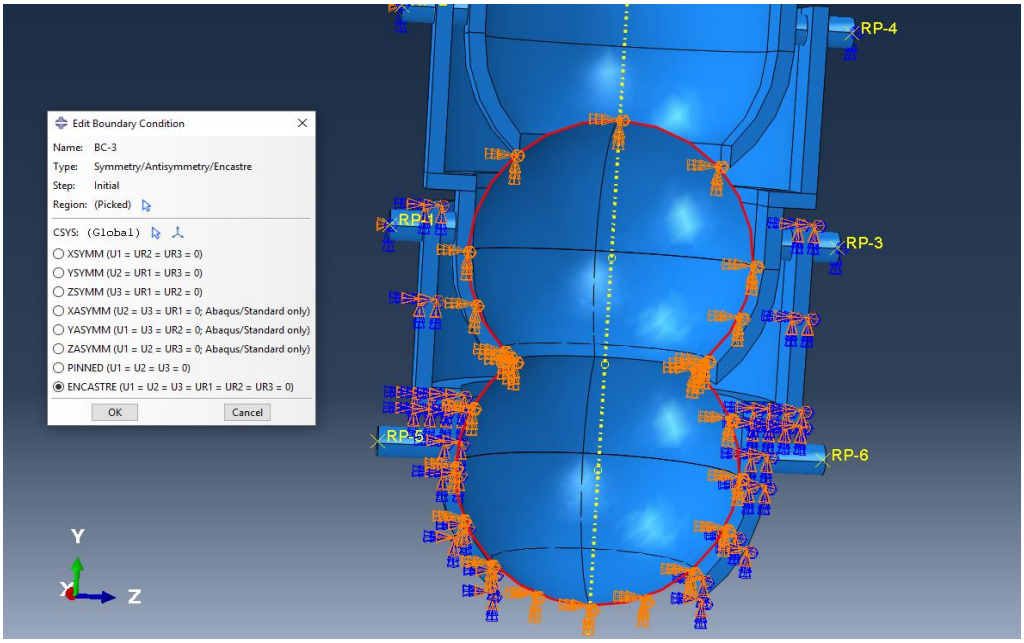

Figure 33 View showing the Pinned surface

3.5 Prototype Manufacturing

This section provides an overview of the process we went through to manufacture the prototype. Manufacturing of this design required three main elements: the shells, the elastomeric inner tube and the assembly components. After the completion of the FEM analysis the CAD Model of the shells was sent for 3D printing. Simultaneously we began the making Models for the three-part mold and also sent them off for 3D printing. It consists of a core, a bottom chamber and a top sliding cover which also acted as a mold for the bottom layer itself.

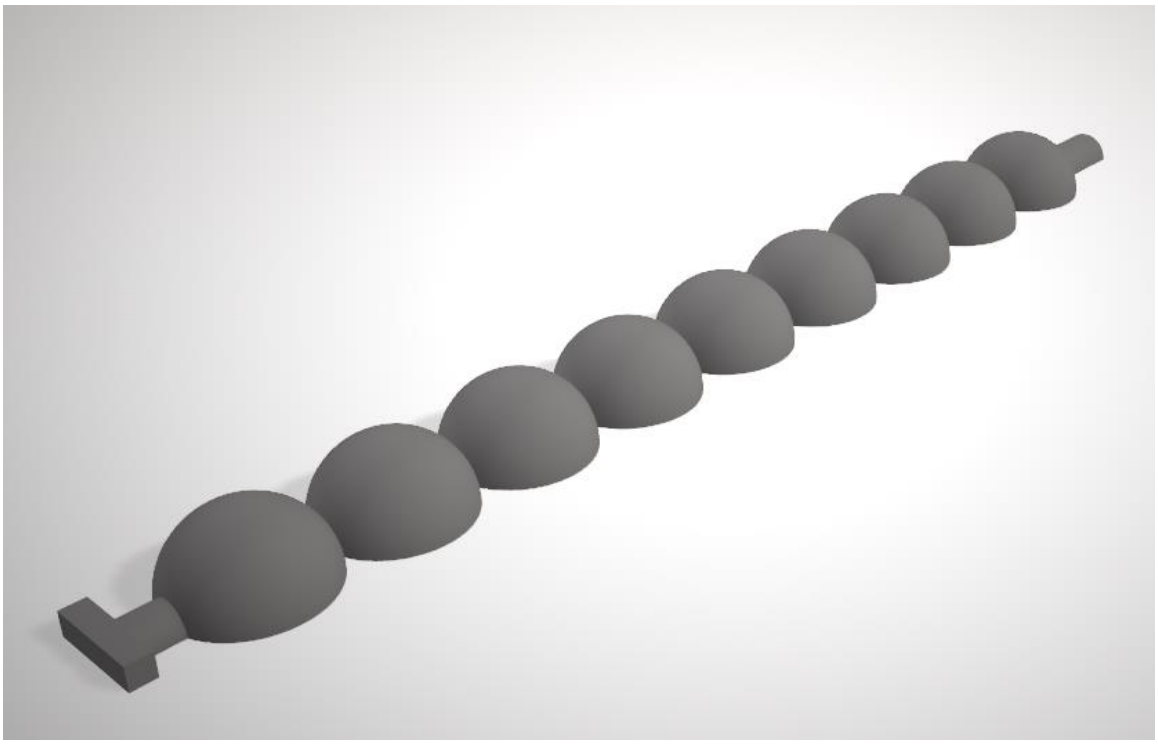

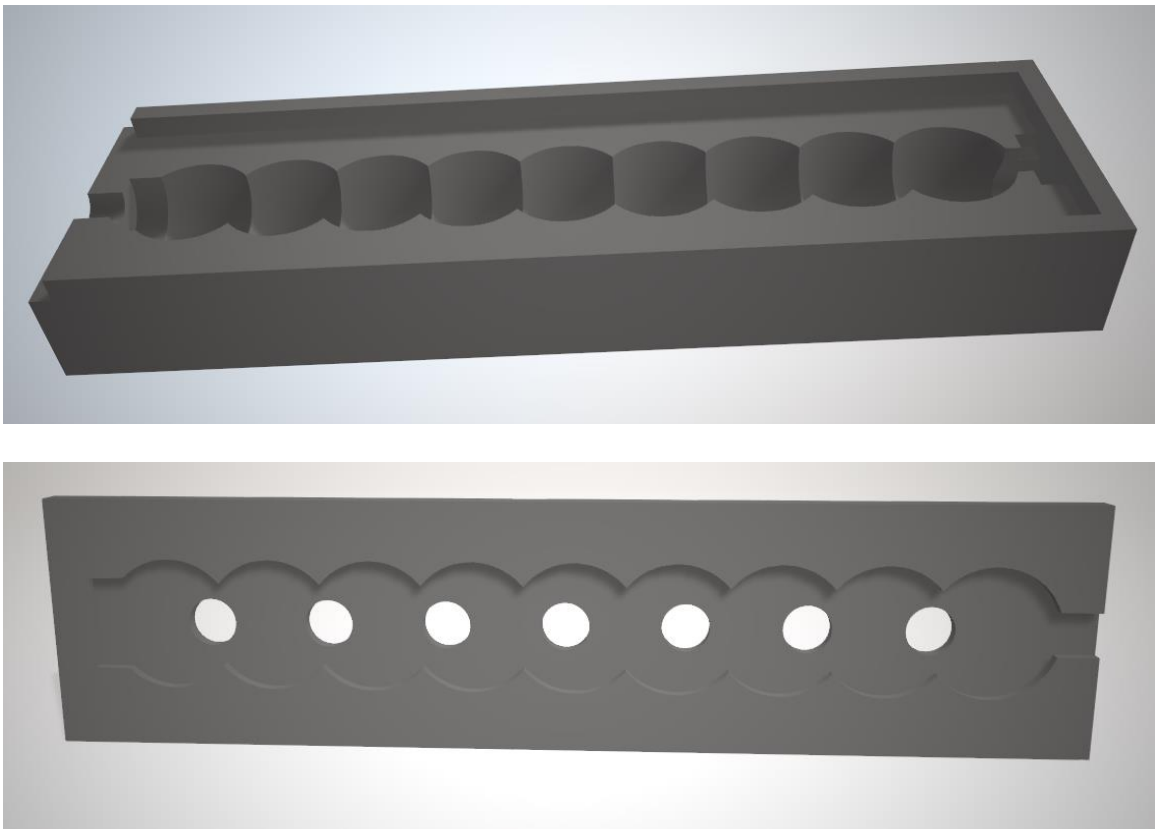

Figure 34 Assembly of Mold (Core, Bottom chamber and Top Cover)

We constructed our own vacuum chamber using house hold item and an acrylic cover. A vacuum pump capable of generating 100kPa of negative pressure was also used.

Figure 35 Image of the Vacuum chamber and Pump

Since the Ecoflex material is cured through additive curing so, extreme care had to be taken during mixing. Also, as industrial level equipment was not being used some defects were anticipated.

This is a two-step molding process. First demolding agent was applied to the core and bottom chamber. Then material component A was poured into a Styrofoam cup after measuring the appropriate amount on the weight balance and specific amount of component B was added to using a dropper with a ratio of 9 to 1 before stirring with a stirrer.

After thorough mixing the material was placed in the vacuum chamber to remove air. This is important because if the air is not removed it leads to the formation of bubbles in the molded material. After removing the air the mixture was poured into the bottom chamber, then the core was placed on top and it was left to cure.

After curing excess material in the form of flanges was removed using clippers. In this way the top layer or top half of the tube was formed. The core was then removed and another batch of the mixture was prepared. The mixture was poured in the mold for the bottom layer and the top layer was placed on top. When the mixture was cured the bottom layer formed was already bonded with the top layer.

After the completion of the molding process the sealing of both sides was done. One side was completely sealed off using sludge of excess material. The other side was closed using a nozzle (connected to a piece of pipe), more excess material and zip ties (to keep the seal).

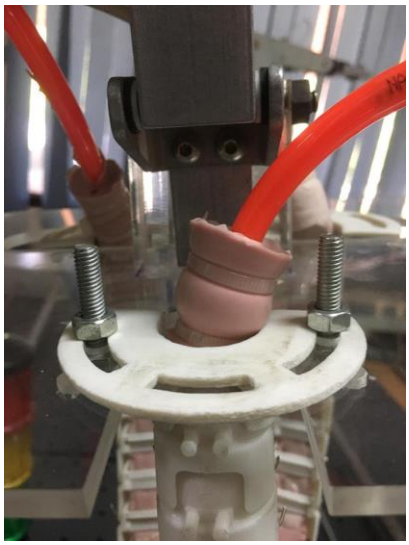

Figure 36 View of the seals on tube

Now the final assembly takes place by attaching the shells one by one and pinning them in place using pins.

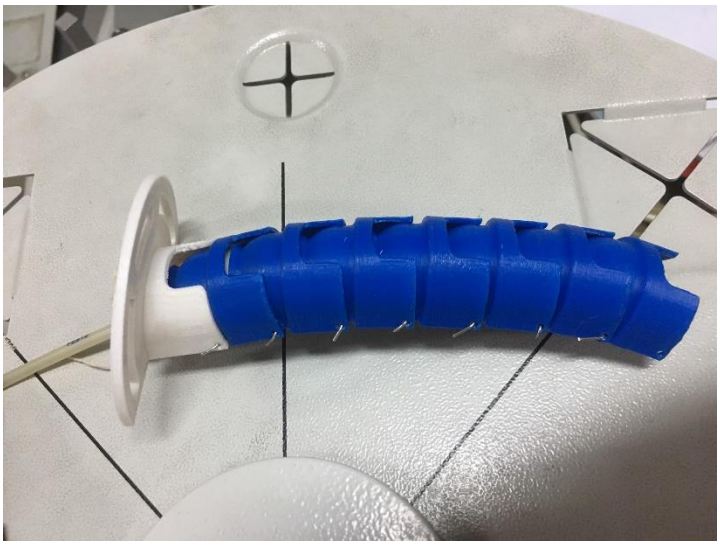

Figure 37 Assembled Prototype

CHAPTER 4: RESULTS AND DISCUSSIONS

This section includes experimental results from the prototype and also the results from the analytical/FEM model solved in ABACUS. It is to be noted that any discrepancies that occurring can be attributed to the simplification of the model.

4.1 Results from FEM Model

The results obtained are as shown. As expected, the tube came in contact with the shell and moment was produced.

The first analysis was done using 3 shells and a two section tube. The section of the assembly is shown as follows. The first shell was encastered as it is the anchoring point of the actuator. A pressure of 150 KPa was applied at the inside of the tube during a time step of 5 seconds. The tube caused the shells to rotate about the pins and the desired motion was obtained. The stresses and forces are as shown. The pin-holes of the first shell had the most stress but was well within the desired limits. The bottom end of the tube is left open for visualization purposes. This model can be extrapolated to 5-7 shells and the actuator can mimic a human finger or a crustacean's leg.

The analysis also highlighted certain factors that could enhance the performance and efficiency which are as follows:

The section between the two shells where the tube inflates and doesn't come in contact with the shell instantly, eventually causes opposite moment. To ensure input pressure contribute to the bending of the shells, the shell geometry is to be designed iteratively.

The figures show the point at which is subjected to the highest stress. The free shell at the other end is subjected to maximum deflection, as desired. The contact stress of the second and the third shell are shown. Further analysis will be carried out once the values from the UTS testing is obtained to model our current elastomer.

4.1.1 Overall Response

The displacement and stresses in the overall actuator are shown below. As can be seen bending was produced as desired.

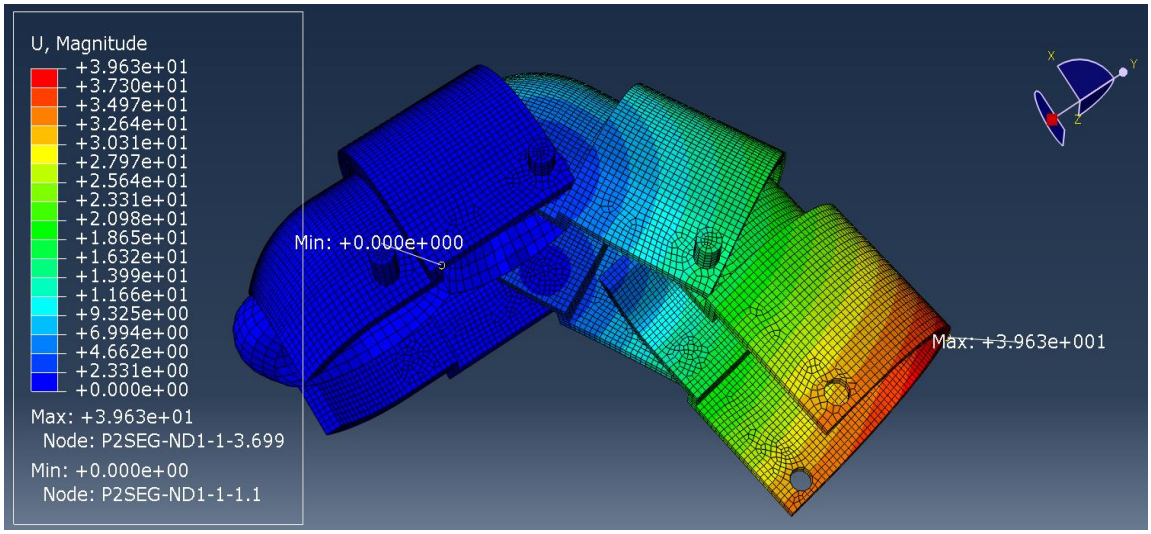

Figure 38 Displacement produced in the actuator. Left most shell is encastered.

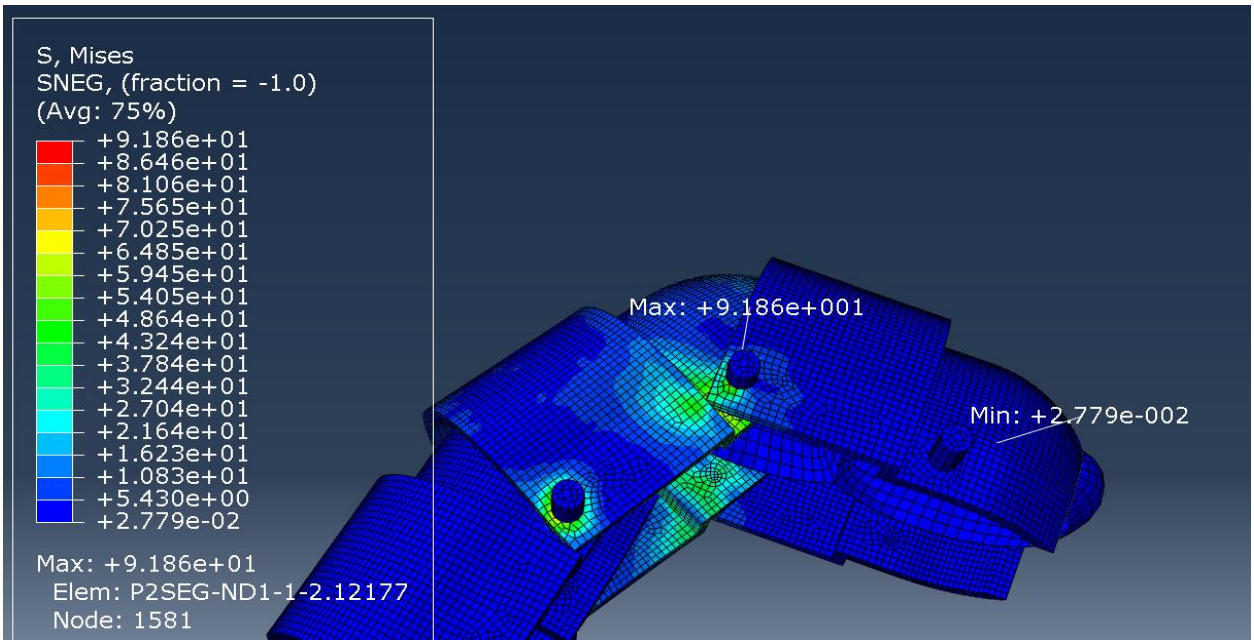

Figure 39 Stresses produced. Highest Stress at the joint between the first and second region

4.1.2 Highest Stress Region-First shell

The highest stress region was at the pin hole of the first shell where it is coupled with the second shell.

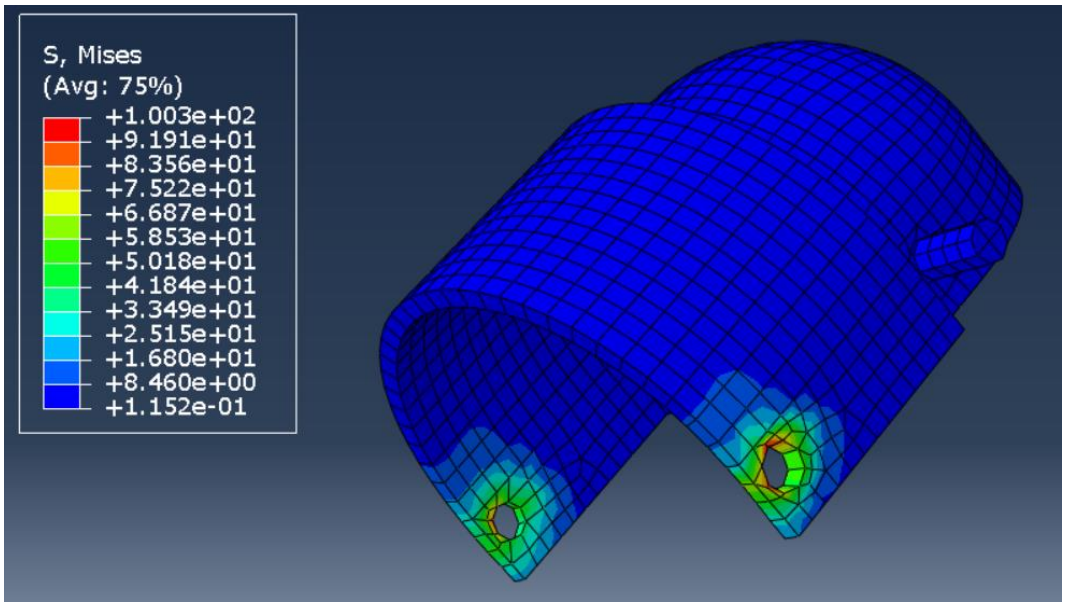

Figure 40 Stresses on the first shell. As expected the highest stress is about the pin holes

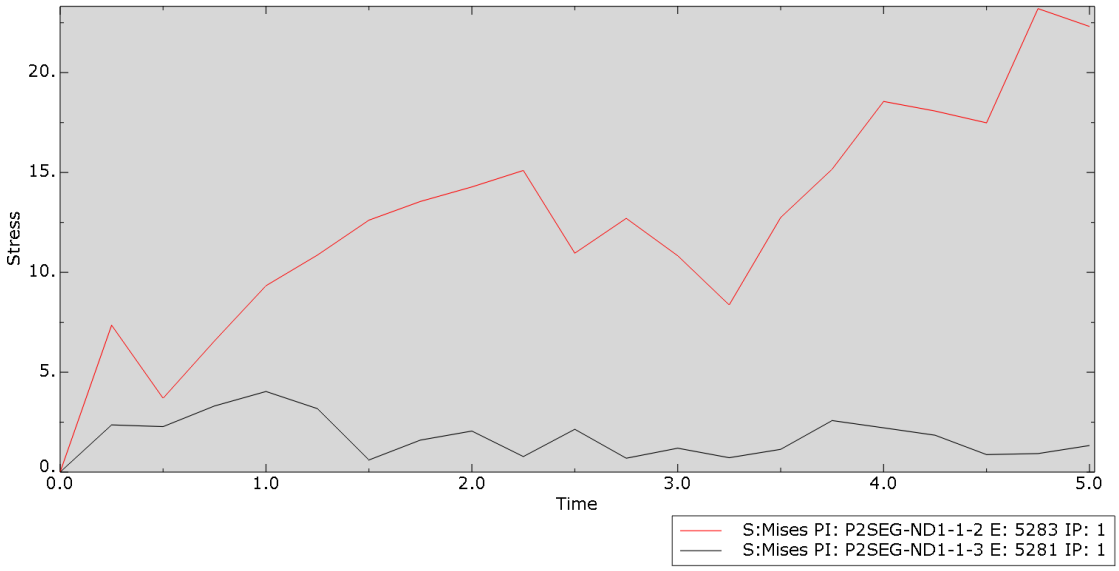

Figure 41 Stress vs Time graph for the highest stress point

4.2 Results from the Prototype Testing

What we aimed for with testing phase was to establish a relation between the input pressure and bending angle. Also, we wanted to establish the loading bearing capabilities and finally we wanted to test one of main features or benefits of this design, that is its shape adaptability or conformability.

4.2.1 Bending Angle vs Pressure

Most soft bodied bending actuators have a limited bending angle they can achieve because beyond that increase in pressure will result in ruptures. A similar case is presented if we try to expand our elastomeric tube without its shells.

But with the addition of shells not only is it protected from the outside but since the tube is constricted within the shells, a higher pressure can be achieved resulting in a larger bending angle. After testing at different pressures, the following data was obtained.

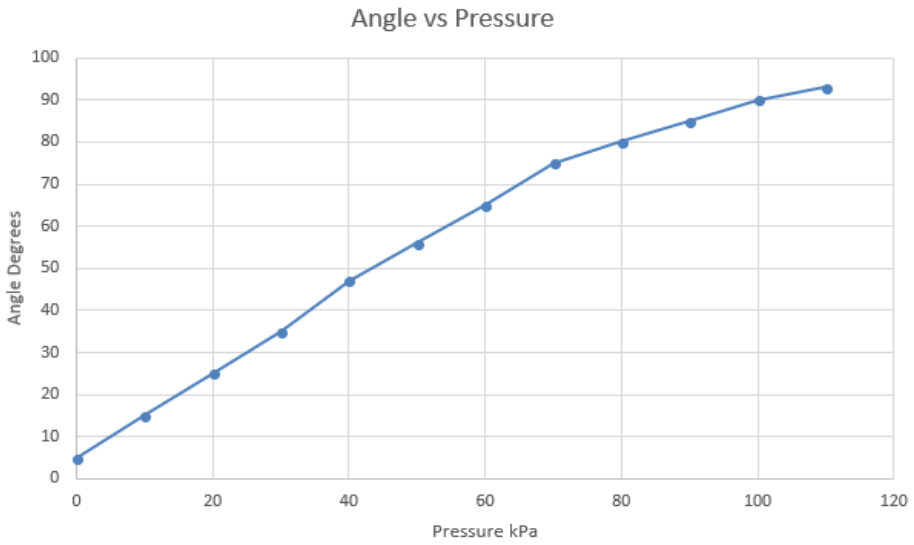

Figure 42 Bending Angle vs Pressure for prototype (with shells)

4.2.2 Maximum Loading Capacity

The maximum loading capacity is determined by finding the point force or the tip force at the end of the actuator. There are many ways to perform this test, we performed it by placing a hook at the end of the actuator and then placing weights at maximum pressure and observing whether adequate bend angle was maintained or not. More weights were then added.

Through this process the maximum loading capacity against the force of gravity was 156g.

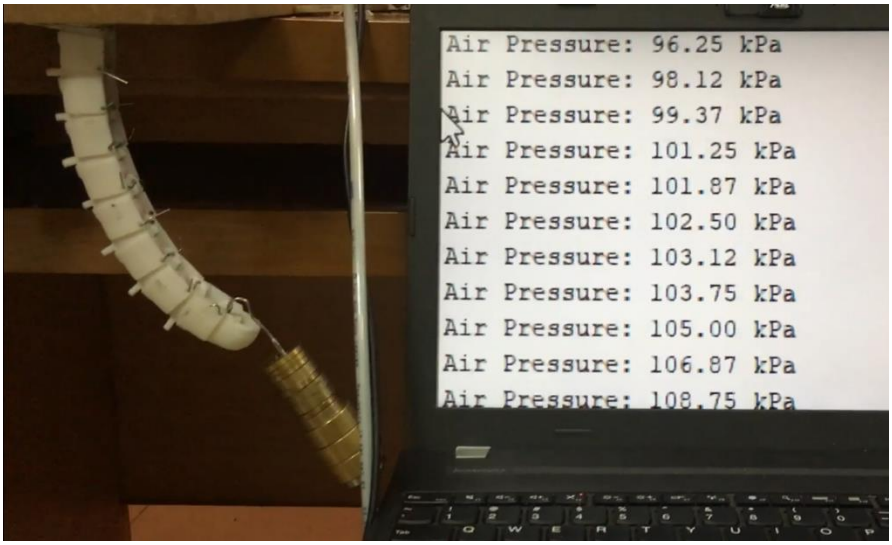

Figure 43 Weight Testing

4.2.3 Shape Adaptability/Conformability

As explained earlier one of the main features of this design is its shape adaptability, how it conforms to changes in geometry (a feature possessed mainly by soft-bodied actuators). In the following images we try to show how this actuator in spite of its rigid elements conforms to different.

Figure 44 Tests for Shape Adaptibility

From the above images we can conclude that the actuator provides sufficient shape adaptability. The shape adaptability can be increased by decreasing the size of shells and increasing their number. However, a balance must be struck between this and

manufacturing cost. As beyond a certain size it is difficult to get good accuracy when manufacturing on a smaller scale using standard equipment.

CHAPTER 5: CONCLUSION AND RECOMMENDATION

5.1 Conclusion

In this project we aimed to design and manufacture a Bio-Inspired Hybrid Muscle which combines the features of rigid and soft bodied mechanisms. We did this by performing a thorough literature review of both soft and rigid actuators. We then developed an initial design based on the limbs of crustaceans. The design was improved and enhanced iteratively using FEM modelling. After finalizing the design we developed a mathematical model for it. Then a prototype was developed for validation of this design and the evaluation of its performance.

Our manufactured prototype achieved a maximum bending angle of 90 degrees forming a U-shape under the action of maximum pressure of 120kPa. It also achieved a maximum pay-load capacity of 156g under the same pressure against the force of gravity.

5.2 Recommendations

At the end of this project we realized that there are still research avenues within the scope of this project. While performing our analysis we observed that varying the dome thickness leads to variation in the expansion of some specific areas. This could possibly be used to avoid the negative torque generated in the mechanism itself.

Variation in shell design or addition of specific flanges could lead to assisting torques not present before. Finally, we applied the hybrid approach on a bending actuator. However, this approach has not yet been implemented on other types of actuators.

Work can also be done to restrict its degrees of freedom through a mechanism which would lead to better gripping and shape adaptability.

5.3 Applications

We have discussed above in general the fields of applications of such an actuator. But we wanted to explore in detail the specific applications this type of design could cater to due to its shape adaptability, smoother actuation rates and controllability.

5.3.1 Gripper (Food-Sorting)

To test and demonstrate the actuator's capabilities as a viable food sorting mechanism we constructed a prototype of an industrial style 3 finger gripper. By taking three of our actuator design prototypes and mounting them in a standard gripping configuration we were able to create an industrial style robot gripper. This end gripper was mounted on top of a robotic arm provided by RISE Lab. The gripper was able to provide adequate gripping. The compliant nature of the actuator ensured that the gripper would adapt to a foreign shape of the object instead of crushing it. Figure 45 shows the single finger curling backward to accommodate the delicate cardboard box even though the mechanism design is trying to curl it in the opposite direction. In a rigid link based mechanism the finger would have retained its shape and position causing the box to be crushed.

Figure 45 Gripper Arrangement

5.3.2 Sixth-Finger (Rehabilitative)

Sixth-Finger is a design application which involves the mounting of the actuator on the wrist which results in the so called sixth-finger, as the actuator acts as a literal sixth-finger. For a person who has suffered a stroke and can't move his hand properly, it would allow him to grip objects and perform basic tasks.

The prototype is still under-construction, we intend to use a brace to attach a mounting shell to the arm in which the actuator will be mounted. And we will use either EMG or EEG signal measuring device to control the actuation so that the patient can control the sixth finger without any external help.

REFERENCES

[1] Gopura, R. A. R. C., et al. "Developments in hardware systems of active upper-limb exoskeleton robots: A review." *Robotics and Autonomous Systems* 75 (2016): 203-220.

[2] Rus, Daniela, and Michael T. Tolley. "Design, fabrication and control of soft robots." *Nature* 521.7553 (2015): 467.

[3] Chen, Yaohui, et al. "A reconfigurable hybrid actuator with rigid and soft components." *Robotics and Automation (ICRA), 2017 IEEE International Conference on*. IEEE, 2017.

[4] Polygerinos, Panagiotis, et al. "Towards a soft pneumatic glove for hand rehabilitation." *Intelligent Robots and Systems (IROS), 2013 IEEE/RSJ International Conference on*. IEEE, 2013.

[5] Polygerinos, Panagiotis, et al. "Soft robotic glove for combined assistance and at-home rehabilitation." *Robotics and Autonomous Systems* 73 (2015): 135-143.

[6] Ogura, Keiko, et al. "Micro pneumatic curling actuator-Nematode actuator." *Robotics and Biomimetics, 2008. ROBIO 2008. IEEE International Conference on*. IEEE, 2009.

[7] Suzumori, Koichi, et al. "A bending pneumatic rubber actuator realizing soft-bodied manta swimming robot." *Robotics and Automation, 2007 IEEE International Conference on*. IEEE, 2007.

[8] Paez, Laura, Gunjan Agarwal, and Jamie Paik. "Design and analysis of a soft pneumatic actuator with origami shell reinforcement." *Soft Robotics* 3.3 (2016): 109-119.

[9] Obiajulu, Steven C., et al. "Soft pneumatic artificial muscles with low threshold pressures for a cardiac compression device." *ASME 2013 International Design Engineering Technical Conferences and Computers and Information in Engineering Conference*. American Society of Mechanical Engineers, 2013.

[10] Mosadegh, Bobak, et al. "Pneumatic networks for soft robotics that actuate rapidly." *Advanced functional materials* 24.15 (2014): 2163-2170.

[11] Nordin, Ili Najaa Aimi Mohd, et al. "3-D finite-element analysis of fiber-reinforced soft bending actuator for finger flexion." *Advanced Intelligent Mechatronics (AIM), 2013 IEEE/ASME International Conference on*. IEEE, 2013.

[12] Polygerinos, Panagiotis, et al. "Modeling of soft fiber-reinforced bending actuators." *IEEE Transactions on Robotics*31.3 (2015): 778-789.

[13] Galloway, Kevin C., et al. "Mechanically programmable bend radius for fiber-reinforced soft actuators." *Advanced Robotics (ICAR), 2013 16th International Conference on*. IEEE, 2013.

[14] Yap, Hong Kai, et al. "A fabric-regulated soft robotic glove with user intent detection using EMG and RFID for hand assistive application." *Robotics and Automation (ICRA), 2016 IEEE International Conference on*. IEEE, 2016.

[15] Bishop-Moser, Joshua, et al. "Design of soft robotic actuators using fluid-filled fiber-reinforced elastomeric enclosures in parallel combinations." *Intelligent Robots and Systems (IROS), 2012 IEEE/RSJ International Conference on*. IEEE, 2012.

[16] Lee, Hyuk Jin, et al. "Development of a patterned parallel pneumatic artificial muscle actuator." *Ubiquitous Robots and Ambient Intelligence (URAI), 2016 13th International Conference on*. IEEE, 2016.

[17] Connolly, Fionnuala, et al. "Mechanical programming of soft actuators by varying fiber angle." *Soft Robotics* 2.1 (2015): 26-32.

[18] https://softroboticstoolkit.com/home

[19] McMahan, William, et al. "Field trials and testing of the OctArm continuum manipulator." *Robotics and Automation, 2006. ICRA 2006. Proceedings 2006 IEEE International Conference on*. IEEE, 2006.

[20] Ogden, Raymond W. *Non-linear elastic deformations*. Courier Corporation, 1997.

[21] https://www.softroboticsinc.com

[22] Mosadegh, Bobak, et al. "Pneumatic networks for soft robotics that actuate rapidly." *Advanced functional materials* 24.15 (2014): 2163-2170.

APPENDIX I: INSTRUMENTS USED

Sr no	Instrument
1	Silicone Gun
2	Jun Air 6-25 SJ27 Air Compressor
3	Stainless Steel Nozzles
4	12V 1/4 inch Solenoid Valves
5	Hand Shear
6	Teflon tape
7	Hand Drill
8	CNC Laser
9	MPX5700AP Air Pressure Sensor
10	Hand saw
11	Vernier Caliper
12	Silicone
13	Elastosil M4601
14	Desktop 3D printer
15	ABS plastic
16	PLA plastic
17	Measuring tape